MULTIPLE DESCRIPTION

LATTICE VECTOR QUANTIZATION

MULTIPLE DESCRIPTION LATTICE VECTOR QUANTIZATION

By

XIANG HUANG, B.ENG.

A Thesis

Submitted to the School of Graduate Studies

In Partial Fulfilment of the Requirements

for the Degree

Master of Applied Science

McMaster University

MASTER OF APPLIED SCIENCE (2006) McMaster University

(Electrical and Computer Engineering) Hamilton, Canada

TITLE: Multiple Description Lattice Vector Quantization

AUTHOR: Xiang Huang, B.Eng. (Huazhong Univ. of Sci. & Tech.)

SUPERVISOR: Dr. Xiaolin Wu

NUMBER OF PAGES: xi, 84

Abstract

This thesis studies the multiple description vector quantization with lattice codebooks (MDLVQ).

The design of index assignment is crucial to the performance of MDLVQ. However, to our best knowledge, none of previous index assignment algorithms for MDLVQ is optimal. In this thesis, we propose a simple linear-time index assignment algorithm for MDLVQ with any $K \geq 2$ balanced descriptions. We prove, under the assumption of high resolution, that the algorithm is optimal for $K = 2$. The optimality holds for many commonly used good lattices of any dimensions, over the entire range of achievable central distortions given the side entropy rate. The optimality is in terms of minimizing the expected distortion given the side description loss rate and given the side entropy rate. We conjecture it to be optimal for $K > 2$ in general.

We also made progress in the analysis of MDLVQ performance. The first exact closed form expression of the expected distortion was derived for $K = 2$. For $K > 2$, we improved the current asymptotic expression of the expected distortion.

Acknowledgement

I would like to take this opportunity to thank many people who made this thesis possible.

First and foremost, I wish to express my appreciation to my supervisor Dr. Wu. His guidance, encouragement and understanding during my research are highly appreciated and will always be remembered.

Special thanks to my readers, Dr. Shirani and Dr. Dumitrescu, for their valuable time. Thanks to Cheryl, Helen, Jill and all other Electrical and Computer Engineering administrative staffs for their friendly assistance.

Sincere thanks to my colleagues Xiaohan, Zhe, Xiangjun, Ning, Nima, Pouya, Ehab, Cindy, Pravesh, Sorina and John at the Multimedia Signal Processing Laboratory, and my roommates Jun, Lin and Zheping. Their help and friendship in the past two years have made my master study enjoyable.

I gratefully dedicate this thesis to my parents, Guoping Huang and Yunzhi Li. Thanks for all their love and support!

Contents

List of Figures

List of Tables

List of Abbreviations

i.i.d.	independent identically distributed
MDC	Multiple Description Coding
MDLVQ	Multiple Description Lattice Vector Quantization
MDSQ	Multiple Description Scaler Quantization
MDVQ	Multiple Description Vector Quantization
pdf	probability density function

Chapter 1

Introduction

1.1 Multiple Description Coding (MDC)

Almost all telecommunication traffics are now carried through data and computer networks. A main advantage of modern packet-switched networks (Figure 1.1) is that they offer server diversity (the possibility of providing a single source through multiple servers) and path diversity (the ability to communicate a content over different paths from a server to a client). An information source can be communicated from multiple servers to multiple clients via different paths in the network. This diversity-based communication paradigm allows more efficient use of network bandwidths and improves robustness against network congestions and channel errors. In order to fully utilize the communication capacity of a network, information senders should choose a network-efficient representation rather than traditional representations used

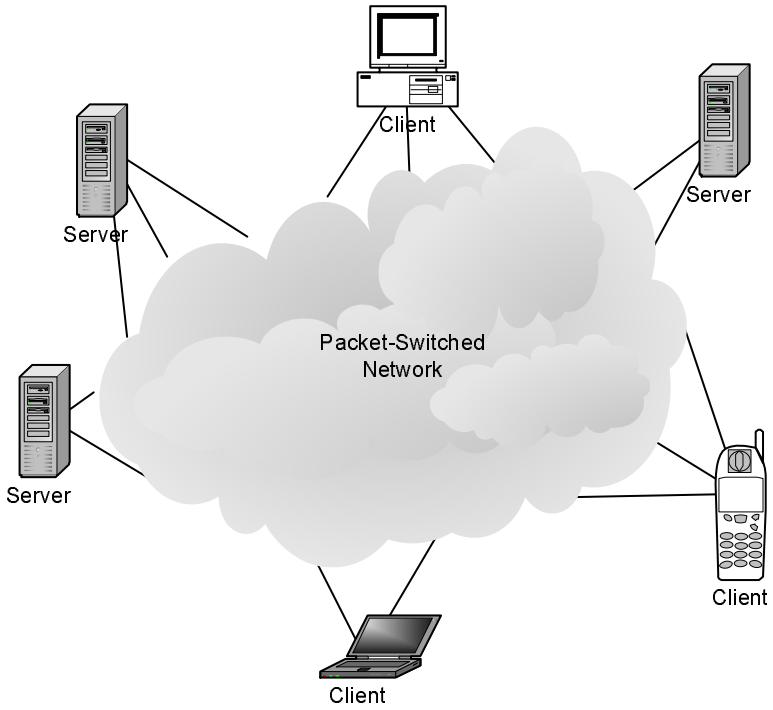

Figure 1.1: Modern Packet-Switched Network

in point-to-point communications. This causes a shift of the methodology of data compression from single code stream from point A to point B via a fixed route to distributed source coding (compression).

Multiple description coding (MDC) is a promising technique for network optimized communications. In particular, it supports error resilient multimedia (image, video, audio, graphics) communications over packet lossy networks such as the Internet and wireless networks. In a packet-switched network, an MDC-coded signal can be transmitted in multiple descriptions via different routes (channels) from one or multiple servers to a receiver. Each description can be independently decoded to a reconstructed signal of certain fidelity, while multiple descriptions can be jointly de-

coded to reconstruct the signal at higher fidelity. The construction fidelity increases in the number of received descriptions. By utilizing path diversity and server diversity, MDC codes can weather adverse network conditions much better than single description codes, particularly in real-time communications where retransmission is not an option. An MDC scheme is depicted in Figure 1.2.

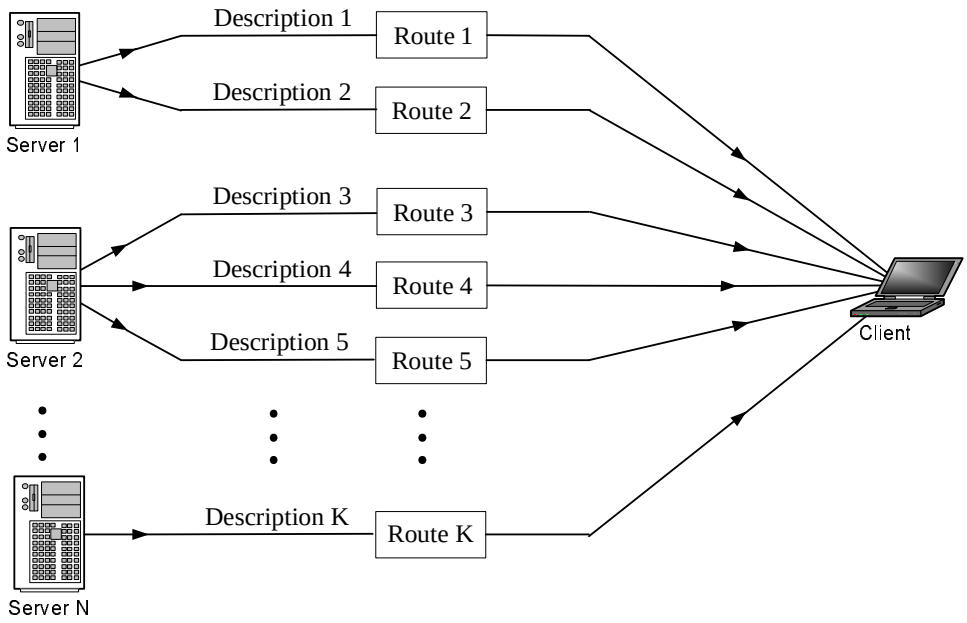

Figure 1.2: Multiple Description Scheme.

1.2 Information Theory Perspective of MDC

Information theory is the foundation of modern digital communications. Shannon first introduced concepts of information theory and established the famous channel

coding theorem and source coding theorems in 1948 [41]. Channel coding is about reliable data transmission over noisy channels. The channel coding theorem defines the channel capacity, which is the maximum information that can be transmitted without error per channel use. Source coding is about lossless or lossy data compression. The source coding theorems give the rate limitations of data compression. In lossless case, the lowest rate is the entropy of the source. In lossy case, the rate-distortion function bounds the lowest rate needed for given distortion.

1.2.1 Introduction to Rate Distortion Theory

MDC generates multiple approximate representations of sources such as image, audio and videos. There is a tradeoff between the lengths of representations (bit rates) and the quality of approximations (distortions). Rate distortion theory discusses the achievable region of rates and distortions. We restate basic concepts of rate distortion theory in this section. For a more systematic treatment of the subject, please refer to Cover and Thomas's book [9].

Assume that a source produces a sequence of independent identically distributed (i.i.d.) random variables $X_1, X_2, \cdots, X_n$. An encoder f maps a source vector $x^n = (x_1, x_2, \cdots, x_n)$ to an index (or codeword) $f(x^n) \in \{1, 2, \cdots, 2^{nR}\}$, where R is bit rate per symbol. A decoder g maps an index from $\{1, 2, \cdots, 2^{nR}\}$ to a reproduction sequence $\hat{x}^n = g(f(x^n))$.

The distortion measure $d(x, \hat{x})$, which is non-negative, evaluates the approxima-

tion between the source sample x and its reproduction $\hat{x}$. The most popular distortion measure is the squared error measure $d(x, \hat{x}) = (x - \hat{x})^2$ due to its simplicity and its relationship to least square prediction. The distortion between sequences $x^n = (x_1, x_2, \cdots, x_n)$ and $\hat{x}^n = (\hat{x}_1, \hat{x}_2, \cdots, \hat{x}_n)$ is defined as the average distortion per symbol, that is

$$d(x^n, \hat{x}^n) = \frac{1}{n} \sum_{i=1}^{n} d(x_i, \hat{x}_i).$$

The distortion associated with the source code (f, g) is defined as the expected distortion between the source and the reproduction:

$$D = E[d(X^n, \hat{X}^n)] = E[d(X^n, g(f(X^n)))].$$

A rate distortion pair (R, D) is said to be achievable if there exits a source code (f, g) with rate R and distortion D for some positive integer n. The closure of the set of achievable rate distortion pairs (R, D) is called the rate distortion region. The rate distortion function $R(D)$ is the infimum of all rates R such that (R, D) is in the rate distortion region for a given D. In dual, the distortion rate function $D(R)$ is the infimum of all distortions D such that (R, D) is in the rate distortion region for a given R.

The main theorem of rate distortion theory states that [9]

$$R(D) = \min_{p(\hat{x}|x): \sum p(x)p(\hat{x}|x)d(x,\hat{x}) \leqslant D} I(X; \hat{X}), \tag{1.1}$$

where the mutual information $I(X; \hat{X})$ is defined as

$$I(X; \hat{X}) \triangleq \sum_{x,\hat{x}} p(x, \hat{x}) \log \frac{p(x, \hat{x})}{p(x)p(\hat{x})}. \tag{1.2}$$

Generally, the rate distortion region is very hard to obtain. For a Gaussian memoryless (i.i.d.) source with variance σ^2, the rate distortion function with squared error measure is given by:

$$R(D) = \begin{cases} \frac{1}{2}\log\frac{\sigma^2}{D}, & 0 \leq D \leq \sigma^2, \\ 0, & D > \sigma^2, \end{cases} \tag{1.3}$$

and the inverse distortion-rate function is:

$$D(R) = \sigma^2 2^{-2R}. \tag{1.4}$$

The Gaussian source is the most difficult source to compress. Among different sources with the same variance, the Gaussian source requires the greatest number of bits to achieve the same distortion. For a memoryless continuous-valued source with variance σ^2 and differential entropy $h(p)$, its distortion rate function with squared error criteria is bounded by [42, 3]:

$$\frac{1}{2\pi e}2^{2h(p)}2^{-2R} \leq D(R) \leq \sigma^2 2^{-2R}, \tag{1.5}$$

where the differential entropy $h(p)$ is determined by the source probability density function $p(x)$,

$$h(p) \triangleq \int p(x)\log_2 p(x)dx. \tag{1.6}$$

For a memoryless Gaussian sources with variance σ^2, we have:

$$h(p) = \frac{1}{2}\log(2\pi e\sigma^2). \tag{1.7}$$

For a memoryless source other than memoryless Gaussian source, the Shannon lower bound $(2\pi e)^{-1}2^{2h(p)}2^{-2R}$ is generally strictly less than $D(R)$ of all $R > 0$, but

it becomes asymptotically tight in the high rate limit [3, 32]:

$$\lim_{R\to\infty} D(R) = \frac{1}{2\pi e} 2^{2h(p)} 2^{-2R}. \tag{1.8}$$

The rate distortion function is often determined by assuming very long block length for encoder, which is not possible in practical codes. However, it is a good analysis of what we can achieve.

1.2.2 Multiple Description Rate Distortion Region

In MDC, each description is associated a rate and each combination of descriptions is associated a distortion. For a K description system, there are K rate parameters and $2^K - 1$ distortion parameters corresponding to $2^K - 1$ combination of descriptions (the case of no description received is trivial). So the rate distortion region for a K description MDC has $K + 2^K - 1$ dimensions, which is very hard to obtain for large K. For simplicity, it is often assumed that the number of descriptions is two, and the multiple description rate distortion region (MD region) is the closure of the sets of achievable rate distortion quintuples $(R_1, R_2, D_1, D_2, D_c)$.

El Gammal and Cover [16] presented an achievable rate distortion region for two description system, which will be referred as the EGC region. The EGC region is not tight: it is not the entire MD region. Zhang and Berger [58] proved there were achievable rate distortion quintuples outside the EGC region, and the EGC region is tight for the case of no excess rate for the joint description, which is when $D_c = D(R_1 + R_2)$. They also provided an improved achievable rate distortion region.

Goyal *et al.* [52] extended the regions of [16, 58] to more than two descriptions. Regions given in [16, 58, 52] generally do not give the entire MD region.

The entire MD region has been known only for Gaussian memoryless sources with squared error measure. The region is first given by Ozarow [37] and is referred to as the Ozarow MD region. Similar to single description, the MD region for any continuous memoryless source with squared error measure can be bounded by the MD region for Gaussian source [57].

For a Gaussian memoryless sources with unit variance and squared error measure, the Ozarow MD region is given by:

$$D_1 \geq 2^{-2R_1}, \tag{1.9}$$

$$D_2 \geq 2^{-2R_2}, \tag{1.10}$$

$$D_c \geq 2^{-2(R_1+R_2)}\gamma, \tag{1.11}$$

where γ is defined as:

$$\gamma \triangleq \begin{cases} 1, & if\ \Pi \leq \Delta \\ \dfrac{1}{1-(\sqrt{\Pi}-\sqrt{\Delta})^2}, & if\ \Pi > \Delta \end{cases}, \tag{1.12}$$

for

$$\Pi \triangleq (1-D_1)(1-D_2)$$

$$\Delta \triangleq D_1 D_2 - 2^{-2(R_1+R_2)}.$$

In the balanced case, where $D_1 = D_2 \triangleq D_s$ and $R_1 = R_2 \triangleq R$, we plot the Ozarow MD region in Figure 1.3. The Ozarow MD region shows some interesting properties

of the achievable MDC performance. At the low side distortion range of the curve, a small increase in side distortion gains a large reduction in central distortion. Similarly, at the low central distortion range of the curve, a small increase in central distortion obtains a large reduction in side distortion.

Three extreme cases will clarify the behavior of the Ozarow MD region. First, consider the balanced case. If each description is individually optimal so that the two side distortions are minimized, that is, $D_1 = D_2 = 2^{-2R}$, then (1.11) becomes $D_c \geq \frac{D_s}{2-D_s}$. The achievable central distortion can not be better than half of the side distortion. For any interesting value of $D_s \ll 1$, this is much greater than the optimal central distortion $D_c = D_s^2$ obtained by (1.4).

The opposite extreme case is when the central distortion is optimized, that is, $D_c = 2^{-2(R_1+R_2)}$. The optimal central description can be achieved only when $\Pi \leq \Delta$ for $\gamma = 1$, which leads to $D_1+D_2 \geq 1+D_c$. So in this case the two side descriptions can not both be optimal: if one side distortion is small (not even necessarily optimal), the other side distortion has to be close to 1, which can be achieved without transmitting any bit in single description system. In the balanced case, both side descriptions need to satisfy $D_s \geq \frac{1+D_c}{2}$, so neither of them can be optimal.

The high-rate case is often studied in information theory for simplification of rate distortion analysis. Under the assumption that $R_1 = R_2 \triangleq R \gg 1$ and $D_1 = D_2 \triangleq D_s \approx 2^{-2R(1-a)}$ with $a \in (0,1)$, we have $\gamma \approx \frac{1}{4D_s}$ and $D_c \geq \frac{1}{4}2^{-2R(1+a)}$. Thus inequality

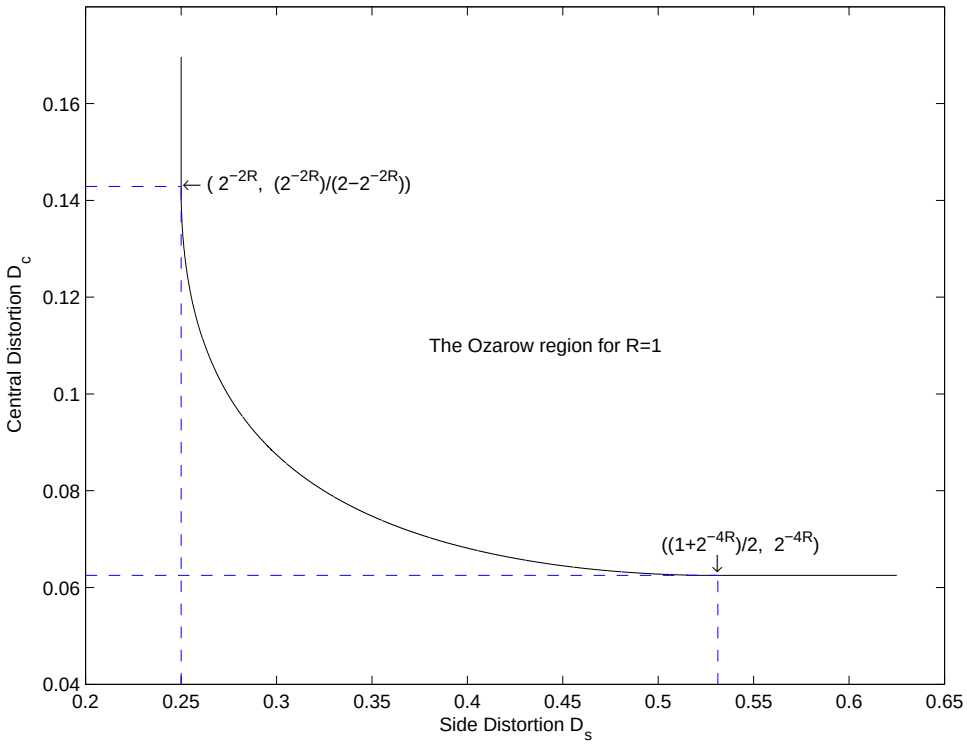

Figure 1.3: The Ozarow MD region for two balanced descriptions.

(1.11) gives

$$\lim_{R\to\infty} D_c D_s \geq \frac{1}{4} 2^{-4R}. \tag{1.13}$$

So in the high-rate balanced case, the product of the central distortion D_c and the side distortion D_s is approximately constant for given R.

1.3 MDC Design Methods

The simplest idea to produce multiple descriptions of the source is by downsampling. We can separate the source into two streams. For instance, odd samples are transmitted over one channel and even samples the other channel. This method was studied

at Bell Laboratories [29] to transmit speech signals on unreliable phone links in 1970s. The practical speech signal is bandlimited to 3.2 kHz and sampled at 8 kHZ. In [29], the initial sampling is at 12 kHz and the downsampling by factor two results only little aliasing. However, this method assume there is redundancy between source samples. But modern compression systems tend to remove redundancy by prediction or decorrelation at the beginning. In these systems, the method by downsampling has poor performance.

Good MDC techniques should not solely rely on the redundancy of the source. They should also be able to introduce different levels of correlation among descriptions by balancing the distortions of central decoder and side decoder according to network statistics. As discussed earlier, the central distortion and side distortion can not achieve minimums simultaneously. Individually optimized descriptions are close to each other and contain a lot of common information, therefore combining those descriptions does not give much performance improvement. To make significant coding gains (lower central distortion) by combining descriptions, different descriptions should contain different information. This implies not all side quantizers can be optimal. A good practical MDC design should produce individually good side descriptions, and at the same time make them different enough to produce a good joint decoder. To balance the performance of central and side decoders, some linear combination of central and side distortions is typically used. The weights can be probabilities of receiving combinations of descriptions. Thus a good MDC design method

should be able to provide the flexibility to optimize for different weights according to different network conditions.

Multiple description codes can be generated by three categories of techniques: quantization, correlating transforms [34, 23, 1, 31], and erasure error correction coding [39, 38]. This thesis is concerned with the first category, which includes MDC approaches based on scalar quantization [48, 50, 43, 44], on trellis coded quantization [28, 53], and on vector quantization [15, 5]. Of particular interest to us is approach of multiple description vector quantization with lattice codebooks [40, 10, 51, 11, 30, 22, 46, 35, 36]. Readers can refer to the survey paper of MDC by Goyal [21] for more details on current MDC methods.

1.3.1 MDC by Quantization

The first practical design of multiple description quantizer was the multiple description scaler quantizer (MDSQ) proposed by Vaishampayan in 1993 [48]. His method allows flexible adjustment of the weighting between central and side distortions. The key mechanism of Vaishampayan's technique is an index assignment (IA) scheme. In the case of two descriptions, the IA scheme labels each codeword of central quantizer by a pair of indices, one for each side quantizer. The process of MDSQ first quantizes a signal sample to a central quantizer codeword, then via index assignment maps this codeword to a pair of side quantizer indices. The two indices are encoded by fixed-length code in [48], so the corresponding scheme is called fixed-rate MDSQ.

The indices can also be encoded by a variable length code [50], the corresponding scheme is called entropy-constrained MDSQ.

For the single description problem, one of the most important results of the quantization theory is that vector quantization is more efficient than scalar quantization, even if the source samples are independent random variables. Why is encoding independent random variables independently not efficient? The answer lies in geometry. In higher dimensions it is possible to construct Voronoi cells that are more spherical than the hypercube. Thus vector quantization offers higher efficiency in space filling, achieving smaller granular distortion than scalar quantization. Through an argument of random quantization [56], it is shown that there exist vector quantizers that approach the rate distortion bound in (1.8). However, uniform scalar quantization with entropy coding at rate R bits per sample has mean squared error[19]

$$\lim_{R\to\infty} D(R) = \frac{1}{12} 2^{2h(p)} 2^{-2R}. \tag{1.14}$$

Thus pontential gain of using vector quantization instead of scalar quantization is $\frac{2\pi e}{12}$, which is well known as the 1.53 dB gain. ($\frac{1}{12}$ and $\frac{1}{2\pi e}$ are respectively the normalized second moments of spheres in one dimensional and infinite dimensional Euclidean spaces.)

Similar to single description system, granular distortion can be reduced by using vector quantization instead of scalar quantization in multiple description system. An high-rate analysis for fixed-rate MDSQ and entropy-constrained MDSQ with uniform central quantizer cells is presented in [47]. In terms of the product of central and

side distortions, there is a gap of 8.69 dB between the fixed-rate MDSQ and the information theory bound of MDC shown in (1.13). For the entropy-constrained MDSQ, the gap shrinks to 3.07 dB. Tian *et al.* proved that by using nonuniform rather than uniform central quantizer cells, the product of central and side distortion can be reduced by 0.4 dB for both fixed-rate and entropy-constrained MDSQ at high rate [45] . These gaps can be closed and the MDC rate distortion bound can be achieved by multiple description vector quantization (MDVQ) with infinite block length [49].

Specifically, for a memoryless source with differential entropy $h(p)$, an entropy-constrained MDSQ with uniform central quantizer cells can achieve [47]

$$\begin{aligned} \lim_{R\to\infty} D_c(R) &= \frac{1}{4}\cdot\frac{1}{12}2^{2h(p)}2^{-2R(1+a)} \\ \lim_{R\to\infty} D_s(R) &= \frac{1}{12}2^{2h(p)}2^{-2R(1-a)}, \end{aligned} \tag{1.15}$$

where $a \in (0,1)$ is a parameter that determines the trade off between the central and side distortions. In contrast, by encoding vectors of infinite block length, it is possible to achieve [49]

$$\begin{aligned} \lim_{R\to\infty} D_c(R) &= \frac{1}{4}\cdot\frac{1}{2\pi e}2^{2h(p)}2^{-2R(1+a)} \\ \lim_{R\to\infty} D_s(R) &= \frac{1}{2\pi e}2^{2h(p)}2^{-2R(1-a)}. \end{aligned} \tag{1.16}$$

Thus MDVQ reduces both side distortion and central distortion by $1.53dB$ from MDSQ.

Theoretically, MDVQ with infinite encoding block length can achieve the MDC rate distortion bound. Unfortunately, optimal MDVQ design is computationally in-

tractable (optimal single-description vector quantization design is already NP-hard [17], which means the computing time for the optimal vector quantizer increases exponentially as the number of codewords increases). To overcome this operational difficulty, a practical and promising way is to use lattice codebooks in vector quantization design [40, 10, 51, 11, 30, 22, 46, 35, 36], which is the case examined by this thesis.

1.3.2 Multiple Description Lattice Vector Quantization (MDLVQ)

A lattice is a regular arrangement of points in space. The motive of using a lattice codebook for vector quantization is to have fast encoding and decoding algorithms [6, 7].

The idea of MDVQ with lattice codebooks was first proposed by Servetto, Vaishampayan and Sloane in 1999 [40], which was often referred as SVS-MDLVQ. The further development and performance analysis of SVS-MDLVQ were presented in [51]. For a memoryless source with differential entropy $h(p)$, the central and side distortions of L-dimensional balanced two-description MDLVQ are:

$$\begin{aligned} \lim_{R\to\infty} D_c(R) &= \frac{1}{4} G_\Lambda 2^{2h(p)} 2^{-2R(1+a)} \\ \lim_{R\to\infty} D_s(R) &= G_L 2^{2h(p)} 2^{-2R(1-a)} \end{aligned}, \tag{1.17}$$

where G_Λ is the normalized second moment of a Voronoi cell of the lattice Λ, G_L is the normalized second moment of an L-dimensional sphere, and $a \in (0, 1)$ is a parameter that determines the trade off between the central and side distortions. Thus the gain

of MDLVQ over MDSQ is G_Λ/G_1 in central distortion, which depends on the lattice, whereas the gain in side distortion is G_L/G_1, which is independent of the lattice.

Similar to the two-description MDSQ scheme in [48, 50], a K-description MDLVQ scheme has two steps: the first step quantizes a source vector to a fine (central) lattice Λ, the second step, via an index assignment (also known as labeling function) α, maps each fine lattice point $\lambda \in \Lambda$ to an ordered K-tuple $(\lambda_1, \lambda_2, \cdots, \lambda_K) \in \Lambda_s^K$, where Λ_s is a coarse lattice. The problem of optimal MDLVQ design involves choosing a lattice Λ for central description and a coarse lattice Λ_s (typically $\Lambda_s \subset \Lambda$, so Λ_s is also called sublattice) for side descriptions, and establishing a one-to-one mapping α between a point $\lambda \in \Lambda$ and an ordered K-tuple $(\lambda_1, \lambda_2, \cdots, \lambda_K) \in \Lambda_s^K$. Given the dimension of source vectors, lattices Λ and Λ_s can be selected from the known optimal and/or near-optimal lattice vector quantizers (e.g., those tabulated in [8]), which have been thoroughly investigated. Therefore, the key issue in optimal MDLVQ design is to find the bijection function $\alpha : \Lambda \leftrightarrow \alpha(\Lambda) \subset \Lambda_s^K$ that minimizes a distortion measure weighted over all possible channel scenarios. This is referred to as the optimal MDLVQ index assignment problem, which is the central theme of this thesis.

The SVS-MDLVQ scheme discussed in [40, 51] was for two balanced descriptions. It is extended to two asymmetric (unbalanced) descriptions in [10, 11]. Kelner,Goyal and Kovačević [30, 22] (KGK-MDLVQ) pointed out the encoding of SVS-MDLVQ was inherently optimized for the central decoder, and the performance can be improved by modifying the encoder and using non-lattices for central decoder (obtained

by slightly modifying the lattices with local training) to minimize the average total distortion. However, the increased complexity by using non-lattices makes the KGK-MDLVQ only feasible for small side-central distortion ratio. Zhao and Kleijin [59] improved the perfomance of KGK-MDLVQ by using a lattice Λ_s for one side description and the translation of Λ_s for the other side description, while the central description codebook is locally trained similarly to KGK-MDLVQ. Tian and Hemami [46] proposed a scheme which favors side quantizers by letting one side quantizer use a lattice codebook, and the other side quantizer use a codebook based on the same lattice with a slight shift. The central quantizer cells is the intersection of Voronoi cells of side quantizers, and a successive refinement stage can be used to further reduce the central distortion. Østergaard *et al.* [35, 36] extended the SVS-MDLVQ to $K \geq 2$ balanced descriptions and presented some asymptotical performance results.

1.4 Contribution and Organization of this Thesis

The design of index assignment is crucial to the performance of the multiple description quantizers. A great deal of efforts were given to optimal IA design, such as the recent works on MDSQ [4, 2], on MDVQ [20], and on MDLVQ [51, 11, 35]. However, to our best knowledge, none of previous IA algorithms is optimal.

The seminal paper of [51] studied the index assignment problem for $K = 2$ balanced MDLVQ in considerable length, and proposed a "guiding principle" for constructing an optimal index assignment for two balanced descriptions. Based on the

guiding principle a good index assignment was given for two balanced descriptions in the A_2 lattice. However, its optimality remained unproven even for the specific instances of MDLVQ. More recently, Ostergaard *et al.* studied the problem of optimal index assignment for $K \geq 2$ balanced MDLVQ, and presented some asymptotical results [35]. The only known solution of optimal MDLVQ index assignment is a linear assignment algorithm about finding a bijective mapping between two infinite sets Λ and Λ_s^K. No good solutions are known to reduce the underlying bipartite graph to a modest size without missing optimal solution. The optimal index assignment algorithm by linear assignment in [35, 36] has extremely high complexity ($O(N^5)$ (N is the sublattice index, which is defined as the ratio of the point densities of central lattice and sublattice) as shown in Section 3.4), and still with no optimality guaranteed.

In this thesis we propose a simple linear-time index assignment algorithm for MDLVQ with any $K \geq 2$ balanced descriptions, and then prove, under the assumption of high resolution, that the algorithm is optimal for $K = 2$ on many commonly used good lattices of any dimensions. The optimality holds over the entire range of achievable central distortions given the side entropy rate, in terms of minimizing the expected distortion given the side description loss rate and given the side entropy rate. We conjecture it to be optimal for $K > 2$ in general. Our results are partly presented in Data Compression Conference 2006 at Snowbird, UT [27].

For the A_2 lattice, the resulting optimal index assignment outperforms the best scheme known so far [51]. Also, for the one-dimensional Z lattice, the optimal index

assignment exhibits the same structures as those suggested first by Vaishampayan for two-description continuous scalar quantization [48], and now widely cited in the literature.

The thesis is structured as follows. After formulating the problem and introducing necessary notations in the next chapter, we propose in Chapter 3 an index assignment algorithm. We analyze the complexity and prove the optimality of the proposed algorithm, and discuss optimal sublattice index N with respect to the probability of description loss in Chapter 3. Chapter 4 presents some new and improved closed form expressions of the expected distortion of optimal MDLVQ, which allow the optimal parameters N and K to be computed. Chapter 5 discusses the codecell convexity of multiple description scalar quantizers, and Chapter 6 concludes.

Chapter 2

Preliminaries

As preparation for presenting our work on multiple description lattice vector quantization, we briefly review mathematical structures of lattices, introduce the K description MDLVQ scheme, derive the rate and distortion expressions of MDLVQ, and formulate the optimal index assignment problem.

2.1 Lattice Vector Quantizer

A lattice Λ in L-dimensional Euclidean space is a discrete set of points. It is defined as

$$\Lambda \triangleq \{\lambda \in \mathbb{R}^L : \lambda = uG, u \in \mathbb{Z}^L\}, \tag{2.1}$$

that is, the set of all possible integral linear combinations of the rows of a matrix G. The $L \times L$ matrix G is called a generator matrix for the lattice. It is full rank.

We define $< x, y >$ as the dimensional-normalized inner product of the L dimen-

sional vectors x and y:

$$\langle x, y \rangle = \frac{1}{L} \sum_{i=1}^{L} x_i y_i.$$

The Voronoi cell of a lattice point $\lambda \in \Lambda$ is defined as

$$V(\lambda) \triangleq \{x \in \mathbb{R}^L : \|x - \lambda\| \leqslant \|x - \tilde{\lambda}\|, \forall \tilde{\lambda} \in \Lambda\}, \tag{2.2}$$

where $\|x\|^2 = \langle x, x \rangle$ is the dimension-normalized norm for vector x.

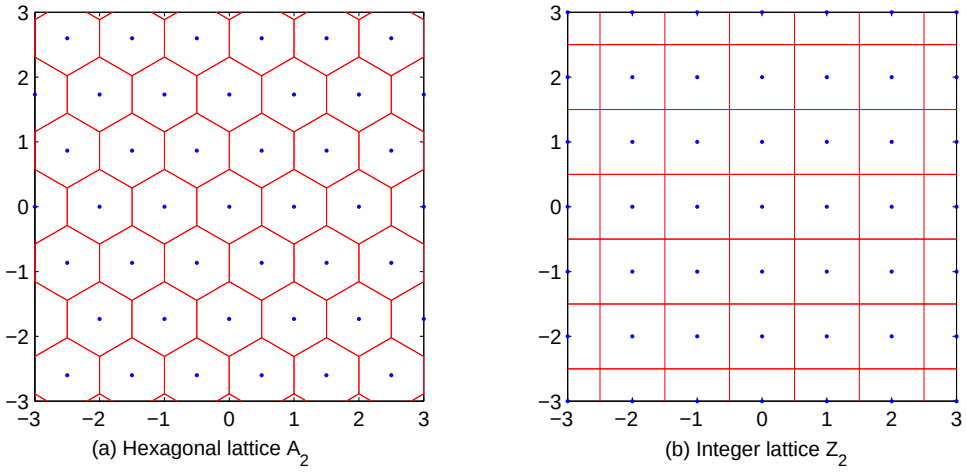

Figure 2.1: Two dimensional lattices A_2, Z^2 and their Voronoi cells.

Figure 2.1 shows examples of hexagonal lattices A_2 and square lattice (two dimensional integer lattice) Z^2. The generator matrix for A_2 lattice is

$$G = \begin{pmatrix} 1 & 0 \\ -\frac{1}{2} & \frac{\sqrt{3}}{2} \end{pmatrix}, \tag{2.3}$$

and for Z_2 lattice is

$$G = \begin{pmatrix} 1 & 0 \\ 0 & 1 \end{pmatrix}. \tag{2.4}$$

All the Voronoi cells of a lattice Λ are congruent. Let ν be the L-dimensional volume of a Voronoi cell . The dimensionless normalized second moment of a lattice Λ is defined by [8]

$$G_\Lambda \triangleq \frac{1}{\nu^{1+2/L}} \int_{V(0)} \|x\|^2 \, dx. \tag{2.5}$$

G_Λ does not depend on the size a Voronoi cell. It only depends on the shape of a Voronoi cell. Thus it is a good evaluation of how sphere like a Voronoi cell is.

A vector quantization scheme with a lattice codebook is called lattice vector quantization [24, 18]. In an L-dimensional lattice vector quantization scheme with codebook Λ, the source samples are first blocked into L-dimensional random vectors, then any random vector $x \in R^L$ is quantized to its nearest lattice point $\lambda \in \Lambda$. The average distortion per dimension of the lattice vector quantizer is given by

$$d_c = \sum_{\lambda \in \Lambda} \int_{V(\lambda)} \|x - \lambda\|^2 \, p_L(x) dx, \tag{2.6}$$

where $p_L(x)$ is the L-fold probability density function (pdf). Under the standard high resolution assumption, each Voronoi cell is small such that $p_L(x)$ is approximately constant in each Voronoi region, thus [8]

$$d_c \approx G_\Lambda \nu^{2/L}. \tag{2.7}$$

2.2 K description MDLVQ

Now we are ready to present the K description MDLVQ scheme. In a K-description MDLVQ, an input vector $x \in R^L$ is first quantized to its nearest lattice point $\lambda \in \Lambda$,

where Λ is a fine lattice. Then the lattice point λ is mapped by a bijective labeling function α to an ordered K-tuple $(\lambda_1, \lambda_2, \cdots, \lambda_K) \in \Lambda_s^K$, where Λ_s is a coarse lattice and Λ_s^K is the Cartesian product of K coarse lattices ($\Lambda_s^K \triangleq \Lambda_s \times \Lambda_s \times \cdots \times \Lambda_s$). Let the components of α be $(\alpha_1, \alpha_2, \cdots, \alpha_K)$, i.e., $\alpha_k(\lambda) = \lambda_k$, $1 \leq k \leq K$. With the function α the encoder generates K descriptions of x: λ_k, $1 \leq k \leq K$, and transmits each description via an independent channel to a receiver.

If the decoder receives all K descriptions, it can reconstruct x to λ with the inverse labeling function α^{-1}. If the decoder receives no descriptions, it reconstructs x by its expected value $E[X]$. In general, due to channel losses, the decoder receives only a subset χ of the K descriptions, then it can reconstruct x to the average of the received descriptions:

$$\hat{x} = \frac{1}{|\chi|} \sum_{\lambda_i \in \chi} \lambda_i.$$

Note the optimal decoder that minimizes the mean square error should decode x to the centroid of the points $\lambda \in \Lambda$ whose corresponding components $\alpha(\lambda)$ equal to χ. But decoding to the average of received descriptions is easy for design [35]. It is also asymptotical optimal for two description case as shown in [51].

A two description MDLVQ system is schematically depicted in Figure 2.2.

2.2.1 Central Lattice and Sublattice

There are two lattices used in the MDLVQ system. The fine lattice Λ is the code book for the central decoder when all the descriptions are received, thus is called

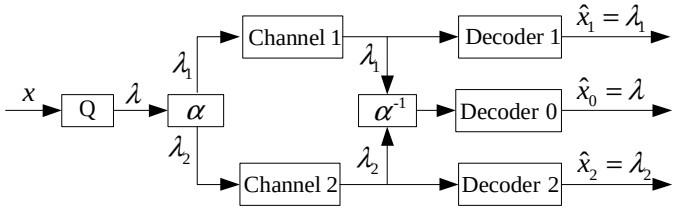

Figure 2.2: MDLVQ scheme with two channels and three receivers.

central lattice. The coarse lattice Λ_s is the code book for a side decoder when only one description is received. Typically, $\Lambda_s \subset \Lambda$, hence Λ_s is called a sublattice. The ratio of the point densities of Λ and Λ_s (which is equal to the ratio of the volumes of the Voronoi cells of Λ_s and Λ) is defined as the sublattice index N. When no central lattice points lie on the boundary of a sublattice Voronoi cell (this is called that the sublattice is clean), N is equal to the number of central lattice points inside a sublattice Voronoi cell. Sublattice index N governs trade-offs between the side and central distortions. We assume that Λ_s is geometrically similar to Λ, i.e., Λ_s can be obtained by scaling, rotating, and possibly reflecting Λ [8]. For simplicity, we will usually assume reflections are not used when we mention Λ_s is geometrically similar to Λ. Figure 2.3 is an example of hexagonal lattice and its sublattice with index $N = 31$.

Let G and G_s be generator matrices for L-dimensional central lattice Λ and sublattice Λ_s. Then Λ_s is geometrically similar to Λ if and only if: there exist an invertible $L \times L$ matrix U with integer entries, a scalar β, and an orthogonal $L \times L$ matrix A

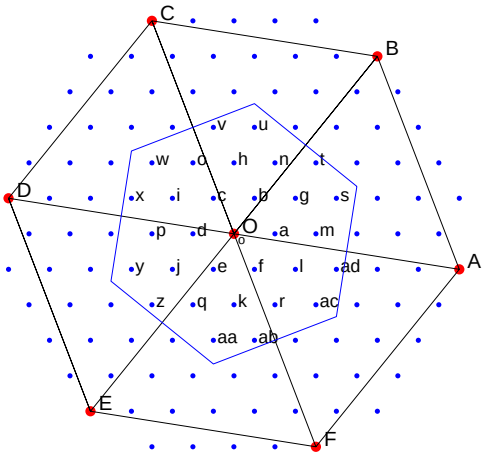

Figure 2.3: Hexagonal lattice A_2 and its sublattice with index $N = 31$. Central lattice points are marked by small dots, and sublattice points by big dots.

with determinant 1 such that

$$G_s = UG = \beta GA, \tag{2.8}$$

The index for a geometrically similar lattice is $N = \frac{detG_s}{detG} = \beta^L$.

In Figure 2.3, the generator matrix for Λ is denoted in (2.3), $\beta = \sqrt{31}$ and

$$G_s = \begin{pmatrix} \frac{11}{2} & -\frac{\sqrt{3}}{2} \\ -2 & 3\sqrt{3} \end{pmatrix}, U = \begin{pmatrix} 5 & -1 \\ 1 & 6 \end{pmatrix}, A = \frac{1}{2\sqrt{31}} \begin{pmatrix} 11 & -\sqrt{3} \\ \sqrt{3} & 11 \end{pmatrix}.$$

2.2.2 Rate of MDLVQ

Assume a information source generates a sequence of independent identically distributed (i.i.d.) random variables with pdf p. The differential entropy rate per dimension of the source is

$$h(p) = \int p(x) \log_2 p(x) dx. \tag{2.9}$$

The source samples are blocked into L-dimensional vectors $x = (x_1, x_2, \cdots, x_L)$. The L-fold pdf is

$$p_L(x) = \prod_{i=1}^{L} p(x_i). \tag{2.10}$$

In MDLVQ, a source vector x is quantized to its nearest fine lattice $\lambda \in \Lambda$. The probability of quantizing to a lattice λ is

$$P(\lambda) = \int_{V(\lambda)} p_L(x)dx. \tag{2.11}$$

We denote by $Q(x) = \lambda$ the quantization mapping. The entropy rate per dimension of the quantizer output is

$$R_c = \frac{1}{L} H(Q(x)), \tag{2.12}$$

where $H(\omega)$ is the entropy function of the discrete random variable ω that takes values in alphabet Ω with probability distribution P,

$$H(\omega) = -\sum_{\omega \in \Omega} P(\omega) \log P(\omega). \tag{2.13}$$

Thus the entropy rate per dimension of the output of the central quantizer is

$$\begin{aligned} R_c &= \frac{1}{L} \sum_{\lambda \in \Lambda} P(\lambda) \log P(\lambda) \\ &= -\frac{1}{L} \sum_{\lambda \in \Lambda} \int_{V(\lambda)} p_L(x)dx \log_2 \int_{V(\lambda)} p_L(x)dx \\ &\approx -\frac{1}{L} \sum_{\lambda \in \Lambda} \int_{V(\lambda)} p_L(x)dx \log_2 p_L(\lambda)\nu \\ &= h(p) - \frac{1}{L} \log_2 \nu., \end{aligned} \tag{2.14}$$

where ν is the volume of a Voronoi cell of Λ. The approximation holds because under high resolution the pdf $p_L(x)$ is approximately constant within an Voronoi cell $V(\lambda)$.

Let R_s be the entropy rate per dimension of an individual description. The volume of a Voronoi cell of the sublattice Λ_s is $\nu_s = N\nu$. Similar to (2.14), we have [51]

$$\begin{aligned} R_s &= \frac{1}{L} H(\alpha_i(Q(X))), 1 \le i \le K \\ &\approx h(p) - \frac{1}{L}\log_2 \nu_s \\ &= h(p) - \frac{1}{L}\log_2 (N\nu). \end{aligned} \tag{2.15}$$

The total entropy rate per dimension for the K description MDLVQ system is

$$R_t = KR_s. \tag{2.16}$$

2.2.3 Distortion of MDLVQ

Assuming that the K channels are independent and each has a probability p to fail, we can write the expected distortion as

$$D = \sum_{k=0}^{K} \binom{K}{k} (1-p)^k p^{K-k} D_k,$$

where D_k is the expected distortion when receiving k out of K descriptions.

For the case of all descriptions received, we have $D_K = d_c$ which is denoted by (2.7). For the case of no descriptions received, we have $D_0 = E[\|X\|^2]$. For the case of only one description received, $D_1 = \frac{1}{K}\sum_{i=1}^{K} d_i$, where d_i is the expected side distortion when only description i is available, that is [51]

$$\begin{aligned} d_i &= \sum_{\lambda\in\Lambda} \int_{V(\lambda)} \|x - \lambda_i\|^2 p_L(x) dx \\ &= \sum_{\lambda\in\Lambda} \int_{V(\lambda)} \left(\|x-\lambda\|^2 + \|\lambda - \lambda_i\|^2 + 2\langle x-\lambda, \lambda - \lambda_i\rangle \right) p_L(x) dx \\ &\approx d_c + \sum_{\lambda\in\Lambda} \|\lambda - \lambda_i\|^2 P(\lambda), \quad 1 \le i \le K \end{aligned} \tag{2.17}$$

The approximation holds because under high resolution assumption λ is the centroid of $V(\lambda)$, thus the term $\int_{V(\lambda)}\langle x-\lambda, \lambda-\lambda_i\rangle p_L(x)dx \approx 0$. Hence the expected distortion when receiving one description is

$$\begin{aligned} D_1 &= \frac{1}{K}\sum_{i=1}^{K} d_i \\ &= d_c + \sum_{\lambda\in\Lambda}\frac{1}{K}\sum_{i=1}^{K}\|\lambda-\lambda_i\|^2 P(\lambda). \end{aligned} \tag{2.18}$$

We denote by m_K the centroid of all K descriptions $\lambda_1, \lambda_2, \cdots, \lambda_K$, that it,

$$m_K \triangleq \frac{1}{K}\sum_{k=1}^{K}\lambda_k. \tag{2.19}$$

Then we have the following equation

$$\begin{aligned} \frac{1}{K}\sum_{i=1}^{K}\|\lambda-\lambda_i\|^2 &= \frac{1}{K}\sum_{i=1}^{K}\|(\lambda-m_K)-(\lambda_i-m_K)\|^2 \\ &= \|\lambda-m_K\|^2 + \frac{1}{K}\sum_{i=1}^{K}\|\lambda_i-m_K\|^2 - \frac{2}{K}\left\langle \lambda-m_K, \sum_{i=1}^{K}(\lambda_i-m_K)\right\rangle \\ &= \|\lambda-m_K\|^2 + \frac{1}{K}\sum_{i=1}^{K}\|\lambda_i-m_K\|^2. \end{aligned} \tag{2.20}$$

Substituting (2.20) into (2.18), we get

$$D_1 = d_c + \sum_{\lambda\in\Lambda}\left(\|\lambda-m_K\|^2 + \frac{1}{K}\sum_{i=1}^{K}\|\lambda_i-m_K\|^2\right)P(\lambda). \tag{2.21}$$

Now we consider the case of receiving $1 < k < K$ descriptions. There are $\binom{K}{k}$ ways of receiving k out of K descriptions. We denote by I the set of all possible combinations of taken k elements out of set $1, \cdots, K$. Then $|\mathrm{I}| = \binom{K}{k}$. Let $\iota =$

$(\iota_1, \iota_2, \cdots, \iota_k)$ be an element of I. Under high resolution assumption, we have [35]

$$\begin{aligned} D_k &= d_c + |\mathrm{I}|^{-1} \sum_{\lambda\in\Lambda} \sum_{\iota\in\mathrm{I}} \left\| \lambda - \frac{1}{k}\sum_{j=1}^{k} \lambda_{\iota_j} \right\|^2 P(\lambda) \\ &= d_c + \sum_{\lambda\in\Lambda} \left(\|\lambda - m_K\|^2 + \frac{K-k}{(K-1)k} \frac{1}{K} \sum_{i=1}^{K} \|\lambda_i - m_K\|^2 \right) P(\lambda), \quad 1 < k < K. \end{aligned} \tag{2.22}$$

Substituting the expressions of D_k into (2.17), we arrive at

$$D = (1-p^K)d_c + \sum_{\lambda\in\Lambda} \left(\zeta_1 \|\lambda - m_K\|^2 + \zeta_2 \frac{1}{K} \sum_{i=1}^{K} \|\lambda_i - m_K\|^2 \right) P(\lambda) + p^K E[\|X\|^2], \tag{2.23}$$

where

$$\begin{aligned} \zeta_1 &= \sum_{k=1}^{K-1} \binom{K}{k} (1-p)^k p^{K-k}, \\ &= 1 - p^K - (1-p)^K \\ \zeta_2 &= \sum_{k=1}^{K-1} \binom{K}{k} (1-p)^k p^{K-k} \frac{K-k}{(K-1)k}. \end{aligned} \tag{2.24}$$

A special case is $K = 2$, where $\zeta_1 = \zeta_2 = 2p(1-p)$ and (2.23) can be simplified to

$$\begin{aligned} D &= (1-p^2)d_c + p(1-p) \sum_{\lambda\in\Lambda} \left(\|\lambda - \lambda_1\|^2 + \|\lambda - \lambda_2\|^2 \right) P(\lambda) + p^2 E[\|X\|^2] \\ &= (1-p^2)d_c + p(1-p) \sum_{\lambda\in\Lambda} \left(2 \left\| \lambda - \frac{\lambda_1 + \lambda_2}{2} \right\|^2 + \frac{1}{2} \|\lambda_1 - \lambda_2\|^2 \right) P(\lambda) + p^2 E[\|X\|^2]. \end{aligned} \tag{2.25}$$

2.3 Optimal Index Assignment Problem

Given source and channel statistics and given total entropy rate R_t, the objective of optimal MDLVQ design is to minimize the expected distortion D by finding optimal

description number K, choosing the best central lattice Λ and sublattices Λ_s (better lattices usually can be chosen in higher dimension but the computational complexity should also be considered), and constructing the optimal index assignment (labeling) function α.

For given description number K and lattices Λ, Λ_s, we reduce the optimal MDLVQ design problem to that of finding the optimal index assignment that minimizes

$$d_s \triangleq \sum_{\lambda \in \Lambda} \left(\frac{1}{K} \sum_{i=1}^{K} \|\lambda_i - m_K\|^2 + \zeta \|\lambda - m_K\|^2 \right) P(\lambda), \tag{2.26}$$

where

$$\begin{aligned} \zeta &\triangleq \frac{\zeta_1}{\zeta_2} \\ &= \frac{\sum_{k=1}^{K-1} \binom{K}{k} (1-p)^k p^{K-k}}{\sum_{k=1}^{K-1} \binom{K}{k} (1-p)^k p^{K-k} \frac{K-k}{(K-1)k}}. \end{aligned} \tag{2.27}$$

When $K = 2$, the objective distortion function can be simplified as:

$$d_s = \sum_{\lambda \in \Lambda} \left(\frac{1}{4} \|\lambda_1 - \lambda_2\|^2 + \left\| \lambda - \frac{\lambda_1 + \lambda_2}{2} \right\|^2 \right) P(\lambda). \tag{2.28}$$

Chapter 3

Index Assignment Algorithm

This section presents a greedy index assignment algorithm for MDLVQ of $K \geq 2$ balanced descriptions. We first reveal some useful lattice structures to be exploited by the index assignment algorithm. Then we describe the greedy index assignment algorithm, analyze its complexity, and prove its optimality for $K = 2$. After that, we present a local adjustment algorithm, and conjecture that a combined use of the greedy algorithm and the local adjustment solves the problem of optimal index assignment for $K \geq 2$. At last we discuss an interesting S-similar property of sublattices that is used in the optimality proof of the greedy algorithm.

3.1 Useful Lattice Properties

In the following study of optimal index assignment for K balanced descriptions, the lattice

$$\Lambda_{s/K} \triangleq \frac{1}{K}\Lambda_s \tag{3.1}$$

plays an important role, and it will be referred as the K-fraction lattice hereafter.

The sublattice Λ_s is the set of all possible integral linear combinations of the rows of its generator matrix G_s:

$$\Lambda_s = \{\lambda_s \in \mathbb{R}^L : \lambda_s = uG_s, u \in \mathbb{Z}^L\}. \tag{3.2}$$

Thus K-fraction lattice can be denoted by:

$$\Lambda_{s/K} = \{\tau \in \mathbb{R}^L : \tau = \frac{u}{K}G_s, u \in \mathbb{Z}^L\}. \tag{3.3}$$

The K-fraction lattice $\Lambda_{s/K}$ has the following interesting relations to Λ and Λ_s.

Property 1. *$m(\lambda_1, \lambda_2, \cdots, \lambda_K) = \frac{1}{K}\sum_{k=1}^{K}\lambda_k$ is an onto (but not one-to-one) map: $\Lambda_s^K \to \Lambda_{s/K}$.*

Proof: 1) $\lambda_1, \lambda_2, \cdots, \lambda_K \in \Lambda_s \Rightarrow \sum_{k=1}^{K}\lambda_k \in \Lambda_s \Rightarrow \frac{1}{K}\sum_{k=1}^{K}\lambda_k \in \Lambda_{s/K}$; 2) $\forall\tau \in \Lambda_{s/K}$, let $\lambda_1 = K\tau, \lambda_2 = \cdots = \lambda_K = 0$, then $\lambda_1, \lambda_2, \cdots, \lambda_K \in \Lambda_s$ and $m(\lambda_1, \lambda_2, \cdots, \lambda_K) = \tau$. ■

This means that the centroid of any K-tuples in Λ_s^K must be in $\Lambda_{s/K}$, and further $\Lambda_{s/K}$ consists only of these centroids.

If two K-fraction lattice points τ_1, τ_2 satisfy $\tau_1 - \tau_2 \in \Lambda_s$, then we say that τ_1 and τ_2 are in the same coset with respect to Λ_s. We note that any K-fraction lattice point belong to one of the K^L cosets.

Property 2. *$\Lambda_{s/K}$ has, in the L-dimensional space, K^L cosets with respect to Λ_s.*

Proof: Let τ_1, τ_2 be two K-fraction lattice points. τ_1, τ_2 can be expressed by

$$\tau_1 = \frac{u}{K} G_s, \ \tau_2 = \frac{v}{K} G_s,$$

where $u = (u_1, u_2, \cdots, u_L) \in \mathbb{Z}^L, v = (v_1, v_2, \cdots, v_L) \in \mathbb{Z}^L$. If and only if u_i and v_i have the same remainder when divided by K for all $i = 1, 2, \cdots, L$, then τ_1 and τ_2 are in the same coset with respect to Λ_s. Because the reminder of an integer divided by K belongs to the K numbers: $(0, 1, \cdots, K-1)$, the K-fraction lattice $\Lambda_{s/K}$ has K^L cosets with respect to Λ_s. ■

The K-fraction lattice $\Lambda_{s/K}$ partitions the space into Voronoi cells. Denote the Voronoi cell of a point $\tau \in \Lambda_{s/K}$ by

$$V_{s/K}(\tau) = \{x : \|x - \tau\| \leq \|x - \tilde{\tau}\|, \forall \tilde{\tau} \in \Lambda_{s/K}\}.$$

For simplicity, we assume that the sublattice is clean, that is, no central lattice points lie on the boundary of the Voronoi region of a sublattice point. (If the sublattice is not clean, we need to break a tie in some prearranged manner on the boundary of a sublattice Voronoi cell.) We can prove that no central lattice points lie on the boundary of any Voronoi cell of the K-fraction lattice, if the sublattice is clean.

Property 3. *$\Lambda_{s/K}$ is clean, if Λ_s is clean.*

Proof: Assume for a contradiction that there was a point $\lambda \in \Lambda$ on the boundary of $V_{s/K}(\tau)$ for a $\tau \in \Lambda_{s/K}$. Scaling both λ and $V_{s/K}(\tau)$ by K places $K\lambda$ on the boundary of $KV_{s/K}(\tau) = \{Kx : \|Kx - K\tau\| \leq \|Kx - K\tilde{\tau}\|, \forall \tilde{\tau} \in \Lambda_{s/K}\}$. But $K\lambda$ is a point of Λ, and $KV_{s/K}(\tau)$ is nothing but the Voronoi cell V_s of the sublattice point $K\tau \in \Lambda_s$, or the point $K\lambda \in \Lambda$ lies on the boundary of $V_s(K\tau)$, contradicting that Λ_s is clean. ■

Property 4. *Both lattices Λ_s and Λ are symmetric about any point $\tau \in \Lambda_{s/2}$.*

Proof: $\forall \tau \in \Lambda_{s/2}$, we have $2\tau \in \Lambda_s$, so $2\tau - \lambda_s \in \Lambda_s$ holds for $\forall \lambda_s \in \Lambda_s$; similarly, $\forall \tau \in \Lambda_{s/2}$, we have $2\tau \in \Lambda$, so $2\tau - \lambda \in \Lambda$ holds for $\forall \lambda \in \Lambda$. ■

3.2 Greedy Index Assignment Algorithm

We are now ready to introduce a greedy index assignment algorithm. We partition the space by Voronoi cells of K-fraction lattice points. For simplicity, we assume the sublattice is clean. (If it is not clean, the algorithm also applies, if we break a tie in some prearranged manner on the boundary of a sublattice Voronoi cell). According to Property 3, no point $\lambda \in \Lambda$ is on the boundary of any Voronoi cell of $\Lambda_{s/K}$. To label the central lattice points inside a Voronoi cell $V_{s/K}(\tau)$, we choose the $|\Lambda \cap V_{s/K}(\tau)|$ nearest ordered K-tuples of sublattice points that have the same centroid τ. It follows from (2.26) that any bijective mapping between the $|\Lambda \cap V_{s/K}(\tau)|$ center lattice points

and the $|\Lambda \cap V_{s/K}(\tau)|$ K-tuples yields the same value of d_s. One can choose an arbitrary assignment between the two sets and still minimize d_s.

According to Property 2, $\Lambda_{s/K}$ has K^L cosets with respect to Λ_s in the L-dimensional space, so there are K^L classes of $V_{s/K}(\tau)$. We only need to label one representative out of each class, and cover the whole space by shifting. Thus it suffices to label a total of N central lattice points.

For the two description case, these $|\Lambda \cap V_{s/2}(\tau)|$ ordered pairs are formed by the $|\Lambda \cap V_{s/2}(\tau)|$ nearest sublattice points to τ in Λ_s by Property 4. Note when $\tau \in \Lambda_s$, the ordered pair (τ, τ) should be used to label τ itself.

3.3 Examples of Greedy Index Assignment Algorithm

Let us see how the greedy labeling works via examples on an A_2 lattice, which are presented graphically in Figure 3.1 and Figure 3.2. The A_2 lattice Λ is generated by basis vectors represented by complex numbers: 1 and $\omega = 1/2 + i\sqrt{3}/2$. By shifting invariance of A_2 lattice, we only need to label the N central lattice points that are belong to K^2 Voronoi cells of $\Lambda_{s/K}$. By angular symmetry of A_2 lattice, we can further reduce the number of points to be labeled.

The first example is a two-description case, with the sublattice Λ_s given by basis vectors $5 - \omega$, $\omega(5 - \omega)$, which is geometrically similar to Λ, has index $N = 31$

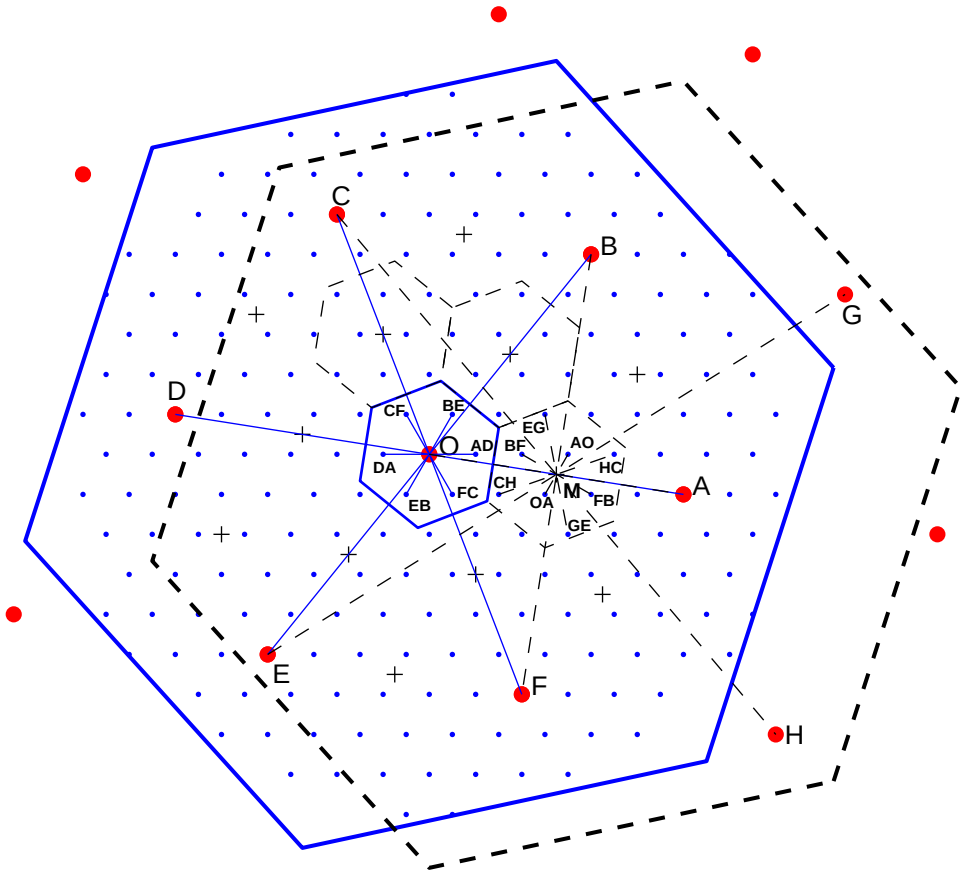

Figure 3.1: Optimal index assignments for A_2 lattice with $N = 31$, $K = 2$. Points of Λ, Λ_s and $\Lambda_{s/2}$ are marked by $\cdot$, $\bullet$ and $+$, respectively.

and is clean (refer to Figure 3.1). There are two types of Voronoi cells of $\Lambda_{s/2}$, as shown by the solid and dashed boundaries in Figure 3.1. The solid cell is centered at a central lattice point and contains 7 central lattice points. The dashed cell is centered at the midpoint of the line segment OA, and contains 8 central lattice points. To label the 7 central lattice points in $V_{s/2}(O)$, we use the 7 nearest sublattice points to O: (O, A, B, C, D, E, F). They form 6 ordered pairs with the midpoint O : $((A, D), (D, A), (B, E), (E, B), (C, F), (F, C)$, and an unordered pair (O, O) since O

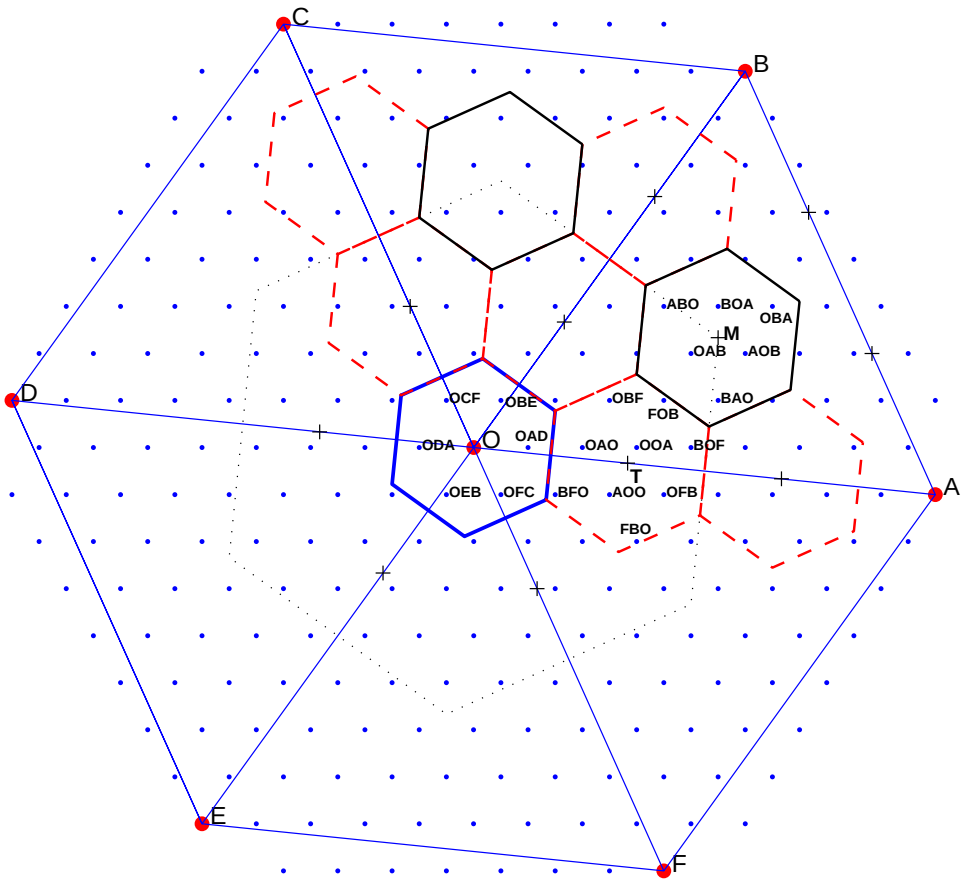

Figure 3.2: Optimal index assignments for A_2 lattice with $N = 73$, $K = 3$. Points of Λ, Λ_s and $\Lambda_{s/3}$ are marked by $\cdot$, $\bullet$ and $+$, respectively.

is itself a sublattice point. To label the 8 central lattice points in $V_{s/2}(M)$, we use the 8 nearest sublattice points to M: (O, A, B, F, C, H, E, G). They form 8 ordered pairs with midpoint M: (O, A), (A, O), (B, F), (F, B), (C, H), (H, C), (E, G), (G, E). The labeling of the 7 central lattice points in $V_{s/2}(O)$ and the labeling of the 8 central lattice points in $V_{s/2}(M)$ are illustrated in Figure 3.1.

Figure 3.2 illustrates how the proposed algorithm works in the case of three de-

scriptions. The depicted index assignment for three balanced descriptions is computed for the sublattice of index $N = 73$ and basis vectors: $8 - \omega$, $\omega(8 - \omega)$.

3.4 Complexity of Greedy Index Assignment Algorithm

The presented MDLVQ index assignment algorithm is fast with an $O(N)$ time complexity. The simplicity and low complexity of the algorithm are due to the greedy optimization approach adopted by it. The tantalizing question is, of course, can the greedy algorithm be optimal? Let the distance between a nearest pair of central lattice points in Λ be one. The result of [51] for the first example (best known so far) is $d_s = 561/31 = 18.0968$, while the greedy algorithm does better, producing $d_s = 528/31 = 17.0323$. Indeed, in both examples, one can verify that the expected distortion is minimized as the two terms of d_s in (2.26) are minimized independently.

In the next section we will prove, under fairly relaxed conditions, that our greedy index assignment algorithm is optimal for two balanced descriptions under mild conditions despite its simplicity.

The only exact algorithm known so far for optimal MDLVQ index assignment is linear assignment. Although applying the linear assignment algorithm to optimize the index assignment is conceptually straightforward, a key algorithmic issue that determines the complexity remains inadequately treated. This is how to reduce the

labeling problem from an association between two infinite sets Λ and Λ_s^K to between two finite sets, and keep these two finite sets as small as possible without compromising optimality.

Diggavi *et al.* proposed a technique of product sublattice to convert the index assignment problem for two description lattice VQ to a bipartite graph matching problem [11]. Two sublattices Λ_1, Λ_2, and their product sublattice of Λ_s are used to construct the two description LVQ. The index assignment is obtained by a minimum weight matching between a Voronoi set of central lattice points and a set of edges (ordered pairs of sublattice points, one end point in Λ_1 and the other in Λ_2). Each set has a cardinality of $N_1 N_2$, where N_k is the index of Λ_k, $k = 1, 2$. Therefore, the index assignment can be computed in $O((N_1 N_2)^{2.5})$ time, given that the weighted bipartite graph matching can be solved in $O(N^{2.5})$ time [26].

Diggavi *et al.* only argued their index assignment algorithm to be optimal for two description lattice scalar quantizers, but did not address the issue of optimality for lattice vector quantizers. This technique of constructing MDLVQ using a product sublattice was generalized from two descriptions to any K balanced descriptions by Østergaard *et al.* [35]. The index assignment solution proposed by [35] seems to require $O(N^5)$ time because it used a candidate set of $O(N^2)$ central lattice points. Even with such a large set of candidate central lattice points, still no bound was given on the size of the candidate K-tuples of sublattice points used for labeling, and no proof of optimality was offered.

3.5 Optimality of Greedy Index Assignment Algorithm

In this subsection we investigate the optimality of the greedy MDLVQ index assignment algorithm proposed above. We start from a good natural construction of sublattice Λ_s.

Definition 1. *A sublattice Λ_s is said to be centric, if the sublattice Voronoi cell $V_s(\lambda)$ centered at $\lambda \in \Lambda_s$ contains the N nearest central lattice points to λ.*

Figure 3.1 and Figure 3.2 show two examples of centric sublattices. Also, it is easy to see that any sublattice of Z lattice is centric.

To prove the optimality of the greedy algorithm, we first introduce some additional properties.

Lemma 1. *Assume the sublattice Λ_s is centric. If $\lambda \in V_{s/2}(\tau)$ and $\tilde{\lambda} \notin V_{s/2}(\tilde{\tau})$, where $\lambda, \tilde{\lambda} \in \Lambda$ and $\tau, \tilde{\tau} \in \Lambda_{s/2}$, then $\|\lambda - \tau\| \leq \|\tilde{\lambda} - \tilde{\tau}\|$.*

Proof: Scaling both λ and $V_{s/2}(\tau)$ by 2 places the lattice point 2λ in $V_s(2\tau)$; scaling both $\tilde{\lambda}$ and $V_{s/2}(\tilde{\tau})$ by 2 places the lattice point $2\tilde{\lambda} \notin V_s(2\tilde{\tau})$. Since a sublattice Voronoi cell contains the nearest central lattice points, $\|2\lambda - 2\tau\| \leq \|2\tilde{\lambda} - 2\tilde{\tau}\|$, and hence $\|\lambda - \tau\| \leq \|\tilde{\lambda} - \tilde{\tau}\|$. ■

Definition 2. *A lattice Λ_s is said to be S-similar to Λ, if Λ_s can be generated by scaling and rotating Λ around any point $\tau \in \Lambda_{s/2}$ and Λ_s is a sublattice of Λ.*

Note the S-similarity requires that the center of symmetry be a point in $\Lambda_{s/2}$.

In what follows we assume that sublattice Λ_s is S-similar to Λ. Also, we denote by V_τ the region created by scaling and rotating $V_{s/2}(\tau)$ around τ.

Lemma 2. *If* $\lambda_s \in V_\tau$ *and* $\tilde{\lambda}_s \notin V_{\tilde{\tau}}$*, where* $\lambda_s, \tilde{\lambda}_s \in \Lambda_s$ *and* $\tau, \tilde{\tau} \in \Lambda_{s/2}$*, then* $\|\lambda_s - \tau\| \leq \|\tilde{\lambda}_s - \tilde{\tau}\|$.

Proof: This lemma follows from Lemma 1 and the definition of S-Similar. ■

Lemma 3. $\forall \tau \in \Lambda_{s/2}$*, the sublattice points in* V_τ *form* $|\Lambda \cap V_{s/2}(\tau)|$ *nearest ordered 2-tuples with their midpoints being* τ*.*

Proof: Letting $\tilde{\tau} = \tau$ in Lemma 2, we see that V_τ contains the $|\Lambda_s \cap V_\tau| = |\Lambda \cap V_{s/2}(\tau)|$ nearest sublattice points to τ. And these sublattice points are symmetric about τ according to Property 4. Thus this lemma holds. ■

Theorem 1. *The proposed greedy algorithm is optimal for* $K = 2$*, if the sublattice is centric and S-Similar to the associated central lattice.*

Proof: By Property 1, for any $\lambda_1, \lambda_2 \in \Lambda_s$, $(\lambda_1 + \lambda_2)/2 \in \Lambda_{s/2}$. Now referring to (2.26), the proposed algorithm minimizes the second term $\sum_{\lambda \in \Lambda} \|\lambda - (\lambda_1 + \lambda_2)/2\|^2 P(\lambda)$ of d_s, since it labels any central lattice point $\lambda \in V_{s/2}(\tau)$ by $(\lambda_1, \lambda_2) \in \Lambda_s^2$, and $(\lambda_1 + \lambda_2)/2 = \tau$.

The algorithm also independently minimizes the first term $\sum_{\lambda \in \Lambda} \frac{1}{4}\|\lambda_1 - \lambda_2\|^2 P(\lambda)$ of d_s. Assume that $\sum_{\lambda \in \Lambda} \|\lambda_1 - \lambda_2\|^2 P(\lambda)$ was not minimized. Then there exists an ordered 2-tuple $(\tilde{\lambda}_1, \tilde{\lambda}_2) \in \Lambda_s^2$ which is not used in the index assignment, and

$\|\tilde{\lambda}_1 - \tilde{\lambda}_2\| < \|\lambda_1 - \lambda_2\|$, where $(\lambda_1, \lambda_2) \in \Lambda_s^2$ is used in the index assignment. Let $\tau = (\lambda_1 + \lambda_2)/2, \tilde{\tau} = (\tilde{\lambda}_1 + \tilde{\lambda}_2)/2$. Since (λ_1, λ_2) is used to label a central lattice point in $V_{s/2}(\tau)$, $\lambda_1, \lambda_2 \in V_\tau$ by Lemma 3. However, $\tilde{\lambda}_1, \tilde{\lambda}_2 \notin V_{\tilde{\tau}}$, otherwise $(\tilde{\lambda}_1, \tilde{\lambda}_2)$ would be used in the index assignment by Lemma 3. So we have $\|\lambda_1 - \tau\| \leq \|\tilde{\lambda}_1 - \tilde{\tau}\|$ by Lemma 2, hence $\|\lambda_1 - \lambda_2\| \leq \|\tilde{\lambda}_1 - \tilde{\lambda}_2\|$, contradicting $\|\tilde{\lambda}_1 - \tilde{\lambda}_2\| < \|\lambda_1 - \lambda_2\|$. ■

Remark 1: A sublattice Voronoi cell being centric is not a necessary condition for the optimality of the greedy algorithm. For instance, for the A_2 lattice generated by basis vectors 1 and $\omega = 1/2 + i\sqrt{3}/2$ and the sublattice of index $N = 91$ that is generated by basis vectors $9 - \omega$, $\omega(9 - \omega)$, a sublattice Voronoi cell does not contain the N nearest central lattices, but the greedy algorithm is still optimal as the two terms of d_s are still independently minimized. This is shown in Figure 3.3.

Remark 2: It is easy to choose a centric sublattice for relatively small N and in high dimensional lattices. For instance, the sublattices of A_2 lattice shown in Figure 3.1, Figure 3.2 and Table 4.1 are centric. And any sublattice of Z lattice is centric.

3.6 Local Adjustment Algorithm

Theorem 1 is concerned with when the two terms of d_s in (2.26) can be minimized independently by the greedy algorithm. While being mostly true for $K = 2$ as stated by the theorem and as we saw in the two examples of Section 3.3, this may not be guaranteed by the greedy algorithm when $K > 2$. Figure 3.4 presents the index assignment generated by the greedy algorithm for $K = 3$ on A_2 lattice. The solution

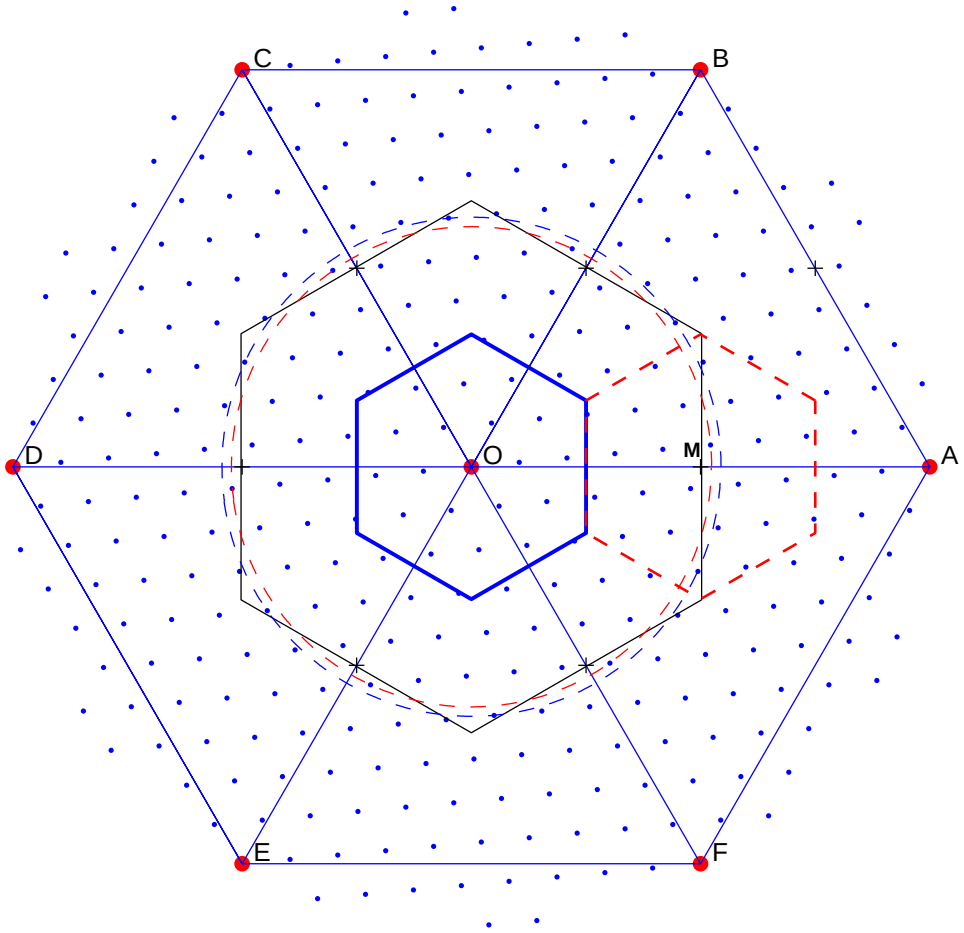

Figure 3.3: The greedy algorithm is optimal for $N = 91$, although the sublattice is not centric. The 19 central lattice points in $V_{s/2}(O)$ are labeled by the 19 nearest ordered 2-tuples with centroid O. The 24 central lattice points in $V_{s/2}(M)$ are labeled by the 24 nearest ordered 2-tuples with centroid M. Let the edge length of 2-tuple (O, A) be one: $||O - A|| \triangleq 1$. The $19th$ $(20th)$ nearest ordered 2-tuple with centroid O has edge length 4 $(2\sqrt{7})$. The $24th$ $(25th)$ nearest ordered 2-tuple with centroid M has edge length 5 $(3\sqrt{3})$. Because $4 < 3\sqrt{3}$ and $5 < 2\sqrt{7}$, the first term of d_s is minimized. The second term of d_s is minimized because the greedy algorithm partition the space by the Voronoi cells of the K-fraction lattice.

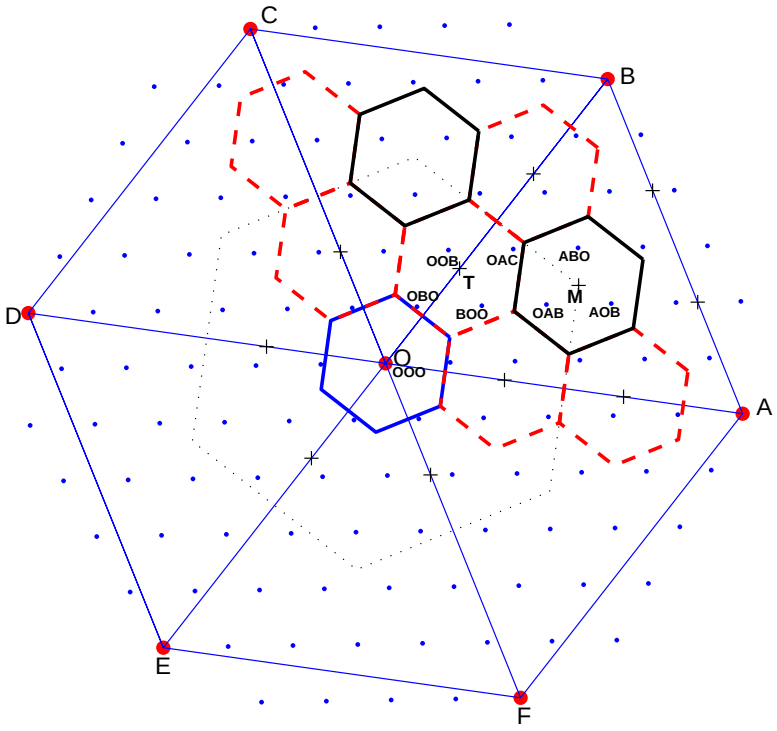

Figure 3.4: Index assignments (not optimal) by the greedy index assignment algorithm for the A_2 lattice with index $N = 31$, $K = 3$. Points of Λ, Λ_s and $\Lambda_{s/3}$ are marked by $\cdot$, $\bullet$ and $+$, respectively.

is now suboptimal. Indeed, consider the central lattice point in $V_{s/3}(T)$ that is labeled by OAC in Figure 3.4, changing the label from OAC to BOA will reduce d_s of the central lattice point in question. The change reduces the first term of d_s, although the second term of d_s increases slightly. Note that the 3-tuple (O, A, C) has centroid T, and the 3-tuple (B, O, A) has centroid M.

In order to make up for the loss of optimality by the greedy algorithm, we develop a local adjustment algorithm. If a central lattice point λ is labeled by an ordered K-tuple that has centroid $\tau \in \Lambda_{s/K}$, we say that λ is attracted by site τ. If two

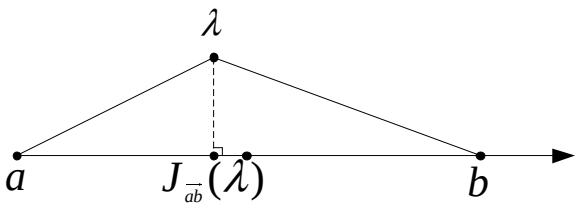

Figure 3.5: Remove lattice λ from site a, and add it to site b

Voronoi cells $V_{s/K}(\tau_1)$ and $V_{s/K}(\tau_2)$ are spatially adjacent, we say that site τ_1 and site τ_2 are neighbors. In Figure 3.4, site O and site T are neighbors, while site O and site M are not neighbors.

In Figure 3.5, assume two neighboring sites a and b attract m and n central lattice points respectively. The m (n) central lattice points are labeled by m (n) nearest ordered K-tuples centered at site a (b). For any point $x \in R^L$, let $J_{\overrightarrow{ab}}(x)$ be the projection value of x onto the axis $\overrightarrow{ab}$. Consider the set $S(a)$ of all the m points currently attracted by site a, and find

$$\lambda_{max} = \arg \max_{\lambda \in S(a)} J_{\overrightarrow{ab}}(\lambda). \tag{3.4}$$

Now, introduce an operator $\vec{\Gamma}\ (a, b)$ that alters the label of λ_{max} to an ordered K-tuple of sublattice points centered at b. The effect of $\vec{\Gamma}\ (a, b)$ is that sites a and b attract $m-1$ and $n+1$ central lattice points respectively, which are respectively labeled by $m-1$ and $n+1$ nearest ordered K-tuples centered at site a and site b.

From the definition of side distortion $d_s = \sum_{\lambda \in \Lambda} d(\lambda)P(\lambda)$ in (2.26), we have

$$d(\lambda) = \left(\frac{1}{K} \sum_{k=1}^{K} \|\alpha_k(\lambda) - m_K\|^2 \right) + \left(\zeta \|\lambda - m_K\|^2 \right). \tag{3.5}$$

Let us compute the change of $d(\lambda_{max})$ caused by the operation $\vec{\Gamma}\ (a, b)$.

The change in the second term of $d(\lambda_{max})$ is

$$\begin{aligned} &\zeta\left(\|\lambda_{max}-b\|^2-\|\lambda_{max}-a\|^2\right) \\ &=\frac{\zeta}{L}\left(\left(J_{\overrightarrow{ab}}(\lambda_{max})-L\,\|b-a\|\right)^2-J_{\overrightarrow{ab}}(\lambda_{max})^2\right). \end{aligned} \tag{3.6}$$

Note the change of the second term is positive if $\lambda_{max} \in V_{s/K}(a)$.

The change in the first term is

$$f_b(n+1)-f_a(m), \tag{3.7}$$

where $f_\tau(i)$ is the i^{th} smallest value of $\frac{1}{K}\sum_{k=1}^{K}\|\lambda_k-\tau\|^2$ over all ordered K-tuples $(\lambda_1,\lambda_2,\cdots,\lambda_K)\in\Lambda_s^K$ such that $m(\lambda_1,\lambda_2,\cdots,\lambda_K)=\tau$.

The net change in $d(\lambda_{max})$ made by operation $\vec{\Gamma}\,(a,b)$ is then

$$\Delta(a,b)=\zeta\left(\|\lambda_{max}-b\|^2-\|\lambda_{max}-a\|^2\right)+f_b(n+1)-f_a(m). \tag{3.8}$$

If $\Delta(a,b)<0$, then $\vec{\Gamma}\,(a,b)$ improves index assignment.

The preceding discussions lead us to a simple local adjustment algorithm:

$(a^*,b^*)=\arg\min_{a\ \text{neighbors}\ b}\Delta(a,b)$;

While $\Delta(a^*,b^*)<0$ do

$\vec{\Gamma}\,(a,b)$;

$(a^*,b^*)=\arg\min_{a\ \text{neighbors}\ b}\Delta(a,b)$.

Note that it is only necessary to invoke the local adjustment $\vec{\Gamma}\,(a,b)$ if the greedy algorithm does not simultaneously minimize the two terms of d_s.

Figure 3.6 shows the result of applying the local adjustment algorithm to the output of the greedy algorithm presented in Figure 3.4. It is easy to prove that the

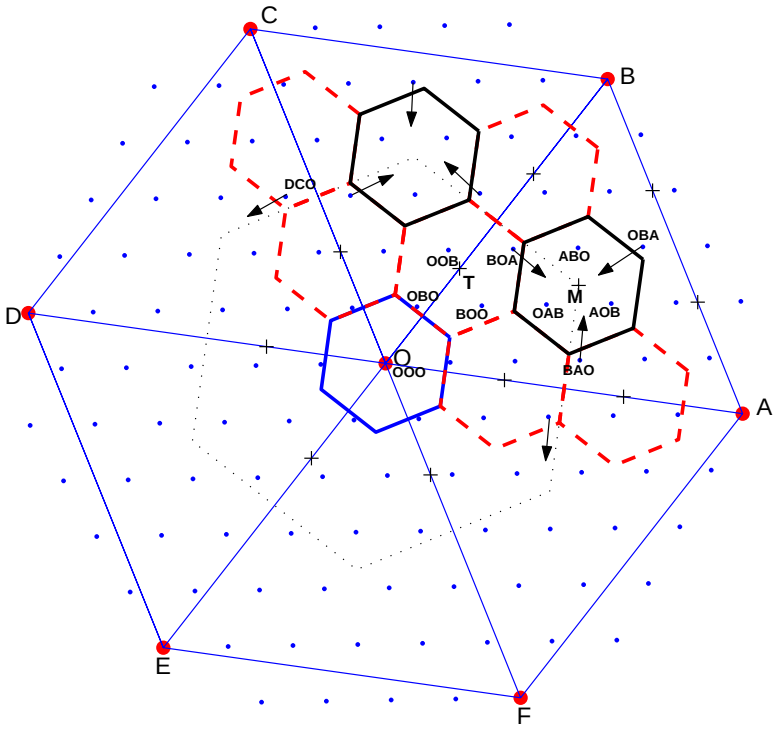

Figure 3.6: Optimal index assignments for the A_2 lattice, $N = 31$, $K = 3$. Points of Λ, Λ_s and $\Lambda_{s/3}$ are marked by $\cdot$, $\bullet$ and $+$, respectively.

local adjustment algorithm indeed finds the optimal index assignment for this case of three description MDLVQ.

Finally, we conjecture that a combined use of the greedy algorithm and local adjustment $\vec{\imath}\ (a, b)$ solves the problem of optimal MDLVQ index assignment for any L-dimensional lattice and for all values of K and N.

3.7 S-Similarity

The proof of algorithm optimality in Section 3.5 requires the S-similarity of the sublattice. In this section we show that many commonly used lattices for signal quantization, such as A_2, Z, Z^2, $Z^L(L = 4k)$, and Z^L (L odd), have S-similar sublattices.

Being geometrically similar is a necessary condition of being S-Similar, but being clean is not (For example a geometrically similar sublattice of A_2 with index 21 is S-Similar but not clean). The geometrical similar and clean sublattices of A_2, Z, Z^2, $Z^L(L = 4k)$, and Z^L (L odd) lattices are discussed in [11]. We will discuss the S-Similar sublattices of these lattices in this section.

Theorem 2. *For the Z lattice Λ, a sublattice Λ_s is S-Similar to Λ, if and only if its index N is odd.*

Proof: Staightforward and omitted. ■

Theorem 3. *For the A_2 lattice Λ, a sublattice Λ_s is S-similar to Λ, if it is geometrically similar to Λ and clean.*

Proof: Let Λ_s be a sublattice geometrically similar to Λ and clean. We refer to the hexagonal boundary of a Voronoi cell in Λ (respectively in Λ_s) as Λ-gon (respectively Λ_s-gon). Any point $\tau \in \Lambda_{s/2}$ is either in Λ_s or the midpoint of a Λ_s-gon edge. For instance, in Figure 3.1 M is both the midpoint of a Λ-gon edge and the midpoint of a Λ_s-gon edge.

If $\tau \in \Lambda_s$, then $\tau \in \Lambda$, hence scaling and rotating Λ around τ yields Λ_s in this case. If τ is the midpoint of a Λ_s-gon edge, then $\tau \notin \Lambda$ because sublattice Λ_s is clean, but $\tau \in \Lambda_{1/2}$, so τ is the midpoint of a Λ-gon edge, hence scaling and rotating Λ around τ yields Λ_s in this case. ■

The $Z^L(L = 4l, l \geq 1)$ lattice has a geometrically similar and clean sublattice with index N, if and only if $N = m^{L/2}$, where m is odd [11]. Here we show that there are S-similar sublattices for at least half of these N values.

Theorem 4. *The $Z^L(L = 4l, l \geq 1)$ lattice Λ has an S-similar, clean sublattice with index N, if $N = m^{L/2}$ with $m \equiv 1 \bmod 4$.*

Proof: We begin with the case $L = 4$. By Lagrange's four-square theorem, there exist four integers a, b, c, d such that $m = a^2+b^2+c^2+d^2$. The matrix G_ξ constructed by *Lipschitz integral quaternions* $\{\xi = a + bi + cj + dk\}$ [11] is

$$G_\xi = \begin{pmatrix} a & b & c & d \\ -b & a & d & -c \\ -c & -d & a & b \\ -d & c & -b & a \end{pmatrix}.$$

The lattice Λ_s generated by matrix $G_s = G_\xi$ is a geometrically similar sublattice of Λ.

Let $\lambda = u$, $\lambda_s = u_s G_\xi$, $\tau = \frac{1}{2} u_\tau G_\xi$ be a point of $\Lambda, \Lambda_s, \Lambda_{s/2}$ respectively, where

$u, u_s, u_\tau \in \mathbb{Z}^L$. Then,

$$\lambda_s - \tau = (u_s - \frac{1}{2}u_\tau)G_\xi.$$

Let $\tilde{u} = u - u_\tau \frac{1}{2}(G_\xi - I_L)$, where I_L is an $L \times L$ identity matrix, then

$$\lambda - \tau = \tilde{u} - \frac{1}{2}u_\tau.$$

Since $n^2 \equiv 1 \bmod 4$ or $n^2 \equiv 0 \bmod 4$ depending on whether n is an odd or even integer, $m \equiv 1 \bmod 4$ implies that exactly one of a, b, c, d is odd. Letting a be odd and b, c, d even, then $\frac{1}{2}(G_\xi - I_L)$ is an integer matrix. Hence $\tilde{u} \in \mathbb{Z}^L$. Thus, scaling and rotating Λ around point τ by scaling factor $\beta = m^{1/2}$ and rotation matrix $A = m^{-1/2}G_\xi$ yields Λ_s, proving Λ_s is S-similar to Λ.

For the dimension $L = 4l, l > 1$, let the $4l \times 4l$ generator matrix of the sublattice Λ_s be

$$G_s = \begin{pmatrix} G_\xi & 0 & \cdots & 0 \\ 0 & G_\xi & \cdots & \vdots \\ \vdots & \vdots & \ddots & 0 \\ 0 & \cdots & 0 & G_\xi \end{pmatrix}.$$

Then Λ_s is S-similar to Λ. And according to [11], Λ_s is clean. ■

The Z_2 lattice Λ has a geometrically similar sublattice Λ_s of index N, if and only if $N = a^2 + b^2, a, b \in \mathbb{Z}$. And a generator matrix for Λ_s is

$$G_s = \begin{pmatrix} a & b \\ -b & a \end{pmatrix}. \tag{3.9}$$

Further, Λ_s is clean if and only if N is odd [11].

Theorem 5. *For the Z_2 lattice Λ, a sublattice Λ_s is S-similar to Λ, if it is geometrically similar to Λ and clean.*

Proof: For a geometrically similar and clean sublattice Λ_s, its generator matrix G_s is given by (3.9). As $N = a^2 + b^2$ is odd, a and b are one even and the other odd. Letting a be odd and b even, by the same argument in proving Theorem 4, scaling and rotating Λ around any point $\tau \in \Lambda_{s/2}$ by scaling factor $\beta = N^{1/2}$ and rotation matrix $A = N^{-1/2}G_s$ yields Λ_s. If a is even, b is odd, scaling and rotating Λ around any point $\tau \in \Lambda_{s/2}$ by scaling factor β and rotation matrix $\tilde{A}$ yields Λ_s, where $\tilde{A}$ is an orthogonal matrix:

$$\tilde{A} = A \begin{pmatrix} 0 & -1 \\ 1 & 0 \end{pmatrix} = N^{-1/2} \begin{pmatrix} b & -a \\ a & b \end{pmatrix}.$$

■

Theorem 6. *An L-dimensional lattice Λ has an S-similar sublattice with index N, if $N = m^L$ is odd.*

Proof: Constructing a sublattice Λ_s with index $N = m^L$ needs only scaling, i.e., $G_s = mG$. Let $\lambda = uG$, $\lambda_s = mu_sG$, $\tau = \frac{1}{2}mu_\tau G$ be in $\Lambda, \Lambda_s, \Lambda_{s/2}$ respectively, where $u, u_s, u_\tau \in \mathbb{Z}^L$. Then,

$$\lambda_s - \tau = m(u_s - \frac{1}{2}u_\tau)G.$$

Let $\tilde{u} = u - \frac{m-1}{2}u_\tau$, then $\tilde{u} \in \mathbb{Z}^L$, and

$$\lambda - \tau = (\tilde{u} - \frac{1}{2}u_\tau)G.$$

Thus, scaling Λ around point τ by $\beta = m^{1/L}$ yields Λ_s, proving Λ_s is S-similar to Λ.

■

Corollary 1. *The Z^L (L is odd) lattice Λ has an S-similar, clean sublattice with index N, if and only if $N = m^L$ is odd.*

Proof: By [11], Λ has a geometrically similar, clean sublattice of index N, if and only if $N = m^L$ is odd. A sublattice Λ_s of this index can be obtained by scaling Λ by m. Theorem 6 implies that Λ_s is S-similar to Λ. ■

Chapter 4

Optimal ν, N and K

In previous discussions, the central lattice Λ and its sublattice Λ_s are fixed, hence the central distortion d_c which is denoted by (2.7) is fixed, and the expected distortion D_k of receiving $k\,(1 \leq k < K)$ descriptions is determined only by the index assignment function α (see (2.22)). The problem of finding the optimal index assignment function α to minimize the expected distortion D at receiving side for given Λ, Λ_s, p and K is discussed in the previous chapter. In this chapter, we fix R_t (the total entropy rate of all side descriptions), and discuss the optimal ν (the volume of a Voronoi cell of Λ), N (the sublattice index) and K (the description number).

4.1 Numerical Results

We begin with two descriptions. According to (2.15), the total entropy rate of two side descriptions $R_t = 2h(p) - \frac{2}{L}\log_2(N\nu)$. We let $(N\nu)^{1/L} = 1$ so that R_t is fixed.

Lattice	L	G_Λ	Admissible N
Z	1	$\frac{1}{12}$	$1, 3, 5, 7, 9, \cdots$
Z^2	2	$\frac{1}{12}$	$1, 5, 9, 13, 17, 25, 29, 37, 41, 45, 49, \cdots$
A_2	2	$\frac{5}{36\sqrt{3}}$	$1, 7, 13, 19, 31, 37, 43, 49, \cdots$

Table 4.1: Index Values for Geometrically Similar and Clean Sublattices

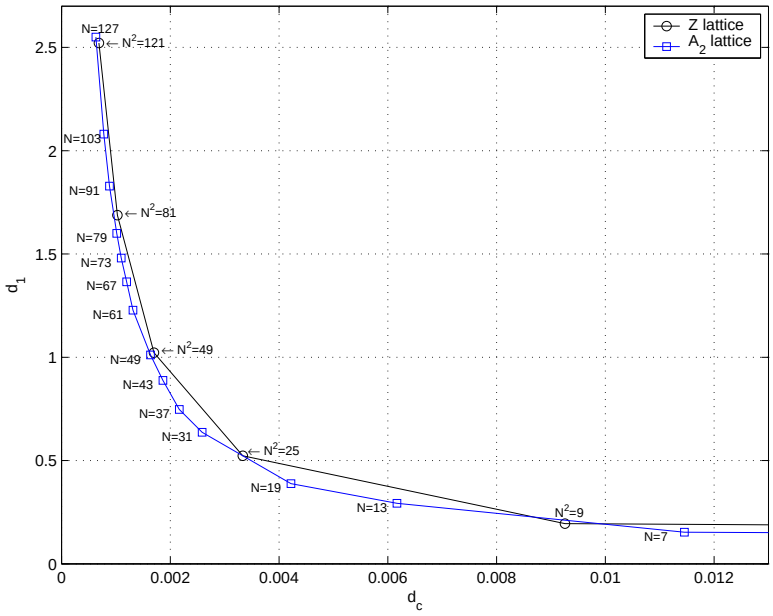

Figure 4.1: d_1 versus d_c for A_2 and Z lattices, where $(N\nu)^{1/L} = 1$.

The sublattice index N governs the trade-off between the side and central distortions. In Table 4.1, the normalized second moments of different lattices are taken from [8], and the admissible index values for geometrical similar and clean sublattices are taken from [11]. Figure 4.1 shows the side distortion d_1 versus the central distortion d_c for A_2 and Z lattices for different sublattice indices N. In case that there are more than one sublattice for the same value of N, we choose the one that gives the

best performance. One can verify that for all the values of N in the

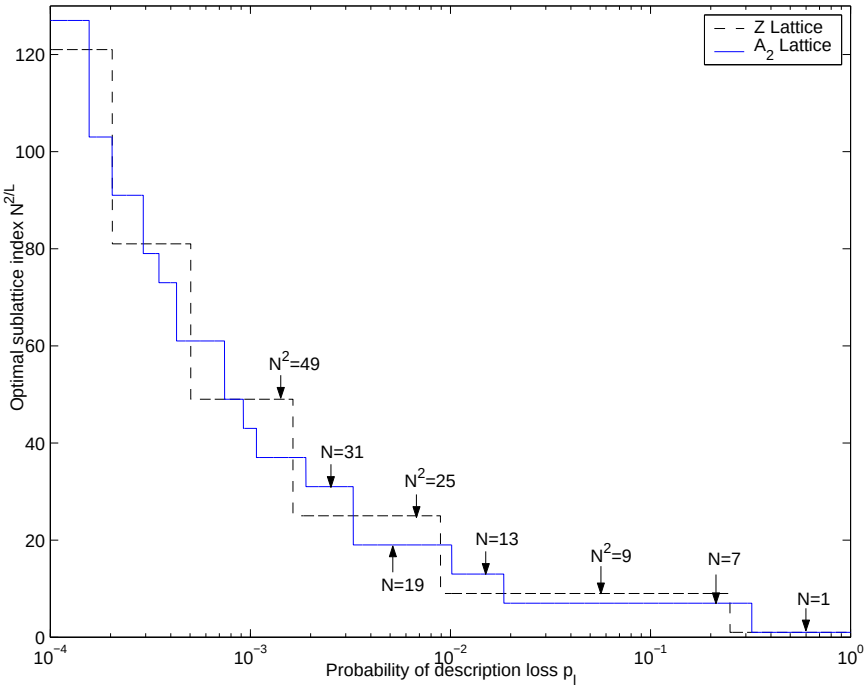

Figure 4.2: Optimal sublattice index values versus description loss probability, $K = 2$

Given the probability of description loss p and the total entropy rate R_t, we can find the optimal sublattice index N_* and the corresponding optimal labeling function α_* so that the expected distortion D in (2.23) is minimized. The optimal sublattice index N_* is independent of R, and depends only on p (decreasing in p). Figure 4.2 plots N_* as a function of p for A_2 and Z lattices. We see that the N_* value remains modest ($N_*^{2/L} < 130$) for a large range of p values ($10^{-4} \leq p \leq 1$).

4.2 Analytical Results for $K = 2$ and Optimal ν, N

Up to now no closed form expression is known for the expected distortion of optimal MDLVQ, except for asymptotic results as $N \to \infty$ [51, 35]. However, practical scenarios for MDLVQ usually involve modest values of N [22]. In this section, we derive the closed form analytical expression of the expected distortion of optimal MDLVQ with two balanced descriptions.

Theorem 7. *If the sublattice is clean and S-similar, then the second term of d_s achieved by our greedy algorithm for two-description MDLVQ is*

$$\sum_{\lambda \in \Lambda} \|\lambda - m_{1,2}\|^2 P(\lambda) = \frac{1}{4L} \frac{\sum_{i=1}^{N} a_i}{N}, \tag{4.1}$$

where a_i is the squared distance of the i^{th} nearest central lattice point in $V_s(0)$ to the origin.

Proof: $\Lambda_{s/2}$ has 2^L cosets with respective to Λ_s in L dimensional space. Let $\tau_1, \tau_2, \cdots, \tau_{2^L}$ be representatives of each coset. For example, when $L = 2$, $\tau_1 = (0,0)G_s, \tau_2 = (0, \frac{1}{2})G_s, \tau_3 = (\frac{1}{2}, 0)G_s, \tau_4 = (\frac{1}{2}, \frac{1}{2})G_s$. We denote by $V_\lambda(\tau) \triangleq V_{s/2}(\tau) \bigcap \Lambda$ the set of central lattice points in the Voronoi cell of a 2-fraction lattice τ. We first prove that

$$2\left(V_\lambda(\tau_i) - \tau_i\right) \bigcap_{i \neq j} 2\left(V_\lambda(\tau_j) - \tau_j\right) = \varnothing. \tag{4.2}$$

$$\bigcup_{i=1}^{2^L} 2\left(V_\lambda(\tau_i) - \tau_i\right) = V_s(0) \cap \Lambda. \tag{4.3}$$

Assume that (4.2) does not hold. Then there exist $\lambda_i \in V_\lambda(\tau_i), \lambda_j \in V_\lambda(\tau_j)$ such that $\lambda_i - \tau_i = \lambda_j - \tau_j$. Let $\tau_0 = \tau_i - \tau_j$, then $\tau_0 \in \Lambda_{s/2}$. We also have $\tau_0 = \lambda_i - \lambda_j$, so

$\tau_0 \in \Lambda$. The sublattice Λ_s is S-similar to Λ, so properly rotating and scaling Λ around the 2-fraction lattice point τ_0 can generate Λ_s. Rotating and scaling the central lattice point τ_0 (remember $\tau_0 \in \Lambda$) around τ_0 itself always generates τ_0, so $\tau_0 = \tau_j - \tau_j \in \Lambda_s$, contradicting τ_i and τ_j are in different cosets with respect to Λ_s. Thus (4.3) holds.

To prove (4.3), we first show that for any $\tau \in \Lambda_{s/2}$,

$$2(V_\lambda(\tau) - \tau) = 2\left(V_{s/2}(\tau) \cap \Lambda\right) - 2\tau = V_s(2\tau) \cap (2\Lambda) - 2\tau \overset{(a)}{\subseteq} V_s(0) \cap \Lambda. \tag{4.4}$$

Step (a) holds because $2\tau \in \Lambda$ and $V_s(2\tau) - 2\tau = V_s(0)$. So we have

$$\bigcup_{i=1}^{2^L} 2\left(V_\lambda(\tau_i) - \tau_i\right) \subseteq V_s(0) \cap \Lambda. \tag{4.5}$$

According to Property 3, no central lattice points lie on the boundary of a K-fraction Voronoi cell when the sublattice is clean, so $\cup_{i=1}^{2^L} V_\lambda(\tau_i)$ contain N different central lattice points. According to (4.2), the set $\cup_{i=1}^{2^L} 2\left(V_\lambda(\tau_i) - \tau_i\right)$ has N different elements. Because the set $V_s(0) \cap \Lambda$ also has N different elements and $\cup_{i=1}^{2^L} 2\left(V_\lambda(\tau_i) - \tau_i\right) \subseteq V_s(0) \cap \Lambda$, (4.3) holds.

Finally, according to (4.2) and (4.3),

$$\begin{aligned}
\sum_{\lambda \in \Lambda} \|\lambda - m_{1,2}\|^2 P(\lambda) &= \frac{1}{4} \sum_{\lambda \in \Lambda} \|2\lambda - 2m_{1,2}\|^2 P(\lambda) \\
&\overset{(a)}{=} \frac{1}{4N} \sum_{i=1}^{4} \sum_{\lambda \in V_\lambda(\tau_i)} \|2\lambda - 2\tau_i\|^2 \\
&= \frac{1}{4N} \sum_{\lambda \in V_s(0) \cap \Lambda} \|\lambda\|^2 \\
&= \frac{1}{4L} \frac{\sum_{i=1}^{N} a_i}{N}.
\end{aligned} \tag{4.6}$$

Equality (a) holds because under high resolution assumption, $P(\lambda)$ is the same for each central lattice point $\lambda \in \cup_{i=1}^{2^L} V_\lambda(\tau_i)$. ■

Theorem 8. *If the sublattice is clean, S-similar and centric, then the closed form expected distortion D of optimal two-description MDLVQ is*

$$D = (1-p^2)G_\Lambda \nu^{2/L} + \frac{1}{2}p(1-p)L^{-1}(1+N^{2/L})N^{-1}\sum_{i=1}^{N} a_i + p^2 E[\|X\|^2]. \qquad (4.7)$$

Proof: If the sublattice is clean, S-similar and centric, the greedy algorithm is optimal according to Theorem 1. The first term of d_s is $N^{2/L}$ times the second term of d_s achieved by our optimal greedy algorithm. Combining with Theorem 7, the first term of d_s is

$$\sum_{\lambda\in\Lambda} \frac{1}{4}\|\lambda_1 - \lambda_2\|^2 P(\lambda) = \frac{N^{2/L}}{4L}\frac{\sum_{i=1}^{N} a_i}{N}. \qquad (4.8)$$

Substituting (2.7), (4.1) and (4.8) into (2.25), we get the closed form expression of the expected distortion D in (4.7). ■

The above equations lead to some interesting observations. When the sublattice is centric, a_i is also the squared distance of the i^{th} nearest central lattice point to the origin. The term $N^{2/L}N^{-1}\sum_{i=1}^{N} a_i$ is the average squared distance of the N nearest sublattice points to the origin, which was also realized by previous authors [51]. The other term $N^{-1}\sum_{i=1}^{N} a_i$ is the average squared distance of central lattice points in $V_s(0)$ to the origin.

The optimal ν and N for a given entropy rate of side descriptions can be solved by combing (4.7) and $R_s = h(p) - \frac{1}{L}\log_2 N\nu$ (shown in (2.15)), rather than solving many instances of index assignment problem for varying N.

4.3 Asymptotical Results for $K \geq 2$ and Optimal ν, N, K

In this section, we will see that our greedy index assignment is asymptotically optimal. Using the greedy index assignment, we derive a closed form expression of the expected distortion of optimal MDLVQ for general $K \geq 2$ asymptotically ($N \to \infty$). Our result improves a similar formula presented in [35, 36] that includes an empirically determined constant. It also allows us to determine the optimal volume of a central lattice Voronoi cell ν, the optimal sublattice index N, as well as the optimal number of descriptions K.

Let N_τ denote the number of central lattice points in $V_{s/K}(\tau)$. As $N \to \infty$, each Voronoi cell of $\Lambda_{s/K}$ contains approximately $N_\tau \approx N/K^L$ central lattice points, which are uniformly distributed in $V_{s/K}(\tau)$ which has volume $N_\tau \nu$. Hence the second term of d_s is

$$\begin{aligned} \zeta \sum_{\lambda \in \Lambda} \|\lambda - m_K\|^2 P(\lambda) &= \zeta G_\Lambda (N_\tau \nu)^{2/L} \\ &\approx \zeta G_\Lambda K^{-2} (N\nu)^{2/L}. \end{aligned} \tag{4.9}$$

To analyze the first term of d_s, we evaluate $\sum_{k=1}^{K} \|\lambda_k - m_K\|^2$ for the N_τ nearest sublattice K-tuples $(\lambda_1, \lambda_2, \cdots, \lambda_K)$ with centroids $m_K = \tau \in \Lambda_{s/K}$. Let

$$f \triangleq \sum_{k=1}^{K} \|\lambda_k - m_K\|^2,$$

$$\varsigma_k \triangleq \sum_{i=1}^{k} \lambda_i, k = 1, 2, \cdots, K,$$

Then

$$\begin{aligned} f &= \sum_{k=1}^{K} \left\| \lambda_k - \frac{1}{K}\varsigma_K \right\|^2 \\ &= \left(\sum_{k=1}^{K-1} \left\| \lambda_k - \frac{1}{K}\varsigma_K \right\|^2 \right) + \left\| \lambda_K - \frac{1}{K}\varsigma_K \right\|^2 \\ &= \left(\sum_{k=1}^{K-1} \left\| \left(\lambda_k - \frac{1}{K-1}\varsigma_{K-1} \right) + \frac{1}{K-1}\left(\varsigma_{K-1} - \frac{K-1}{K}\varsigma_K \right) \right\|^2 \right) + \left\| \varsigma_{K-1} - \frac{K-1}{K}\varsigma_K \right\|^2 \\ &\overset{(a)}{=} \left(\sum_{k=1}^{K-1} \left\| \lambda_k - \frac{1}{K-1}\varsigma_{K-1} \right\|^2 \right) + \frac{K}{K-1}\left\| \varsigma_{K-1} - \frac{K-1}{K}\varsigma_K \right\|^2 \\ &\overset{(b)}{=} \sum_{k=1}^{K-1} \frac{k+1}{k}\left\| \varsigma_k - \frac{k}{k+1}\varsigma_{k+1} \right\|^2. \end{aligned} \tag{4.10}$$

Equality (a) holds because the term $\left\langle \sum_{k=1}^{K-1} \left(\lambda_k - \frac{1}{K-1}\varsigma_{K-1} \right), \frac{1}{K-1}\left(\varsigma_{K-1} - \frac{K-1}{K}\varsigma_K \right) \right\rangle$ is equal to zero. After using the same deduction $K-1$ times, we arrive at equality (b).

There is a one-to-one correspondence between $(\lambda_1, \lambda_2, \cdots, \lambda_K)$ and $(\varsigma_1, \varsigma_2, \cdots, \varsigma_K)$. So the problem of finding N_τ nearest sublattice K-tuples $(\lambda_1, \lambda_2, \cdots, \lambda_K)$ with given centroid $m_K = \tau \in \Lambda_{s/K}$, is equivalent to finding the N_τ optimal sublattice $(K-1)$-tuples $(\varsigma_1, \varsigma_2, \cdots, \varsigma_{K-1})$ given $\varsigma_K = K m_K$ in (4.10).

The i^{th} nearest sublattice point to $\frac{k}{k+1}\varsigma_{k+1}$ is approximately on the boundary of an L dimensional sphere with volume $iN\nu$. So given ς_{k+1}, the i^{th} smallest value of $\|\varsigma_k - \frac{k}{k+1}\varsigma_{k+1}\|^2$ is approximately $(iN\nu/B_L)^{2/L}/L = G_L(1+2/L)(iN\nu)^{2/L}$, where $B_L = G_L^{-L/2}(L+2)^{-L/2}$ is the volume of an L-dimensional sphere of unit radius [51], and G_L is the dimensionless normalized second moment of an L-dimensional sphere.

Let f take on its n^{th} smallest value $f^{(n)}$ at $(\varsigma_1^{(n)}, \varsigma_2^{(n)}, \cdots, \varsigma_{K-1}^{(n)})$, and let the sum $\sum_{k=1}^{K-1} \frac{k+1}{k}(i_k)^{2/L}$ take on its n^{th} smallest value at $(i_1^{(n)}, i_2^{(n)}, \cdots, i_{K-1}^{(n)}) \in \mathbb{Z}^{K-1}$. Then

$$\begin{aligned} f^{(n)} &= \sum_{k=1}^{K-1} \frac{k+1}{k} \left\| \varsigma_k^{(n)} - \frac{k}{k+1} \varsigma_{k+1}^{(n)} \right\|^2 \\ &\approx G_L \left(1 + 2/L\right) (N\nu)^{2/L} \sum_{k=1}^{K-1} \frac{k+1}{k} (i_k^{(n)})^{2/L}. \end{aligned}$$

Hence,

$$\begin{aligned} \sum_{\lambda \in \Lambda} \sum_{k=1}^{K} \|\lambda_k - m_K\|^2 P(\lambda) &= \sum_{\tau \in \Lambda_{s/K}} \sum_{\lambda \in V_{s/K}(\tau)} \sum_{k=1}^{K} \|\lambda_k - m_K\|^2 P(\lambda) \\ &\approx \frac{1}{N_\tau} \sum_{n=1}^{N_\tau} \sum_{k=1}^{K-1} \frac{k+1}{k} \left\| \varsigma_k^{(n)} - \frac{k}{k+1} \varsigma_{k+1}^{(n)} \right\|^2 \\ &\approx G_L (1 + 2/L) \left(N\nu\right)^{2/L} \frac{1}{N_\tau} \sum_{n=1}^{N_\tau} \sum_{k=1}^{K-1} \frac{k+1}{k} (i_k^{(n)})^{2/L} \end{aligned} \tag{4.11}$$

Consider the region defined as

$$\Omega \triangleq \left\{ \sum_{k=1}^{K-1} \frac{k+1}{k} x_k^{2/L} \leq C, x_1, x_2, \cdots, x_{K-1} \geq 0, x_1, x_2 \cdots, x_{K-1} \in \mathbb{R} \right\}. \tag{4.12}$$

Chose C appropriately so that the volume of Ω is $V(\Omega) = N_\tau$. As $N_\tau \to \infty$, Ω contains approximately N_τ optimal integer vectors $(i_1, i_2, \cdots, i_{K-1})$. These N_τ points are uniformly distributed in Ω, with density one point per unit volume. Because the ratio between the volume of each point occupied and the total volume is $1/N_\tau$, which approaches zero when $N_\tau \to \infty$, we can replace the summation by integral and get

$$\begin{aligned} \frac{1}{N_\tau} \sum_{n=1}^{N_\tau} \sum_{k=1}^{K-1} \frac{k+1}{k} (i_k^{(n)})^{2/L} &\approx \frac{\int_{x \in \Omega} \sum_{k=1}^{K-1} \frac{k+1}{k} x_k^{2/L} \, dx}{\int_{x \in \Omega} dx} \\ &= \frac{\int_{y \in \Omega_0} \sum_{k=1}^{K-1} y_k^{2/L} \, dy}{\int_{y \in \Omega_0} dy}, \end{aligned} \tag{4.13}$$

where $y_k = (\frac{k+1}{k})^{L/2} x_k, k = 1, 2, \cdots, K-1$, and Ω_0 is defined as

$$\Omega_0 \triangleq \left\{ \sum_{k=1}^{K-1} y_k^{2/L} \leq C, y_1, y_2, \cdots, y_{K-1} \geq 0, y_1, y_2 \cdots, y_{K-1} \in \mathbb{R} \right\}. \tag{4.14}$$

Substituting (4.13) in to (4.11), we have

$$\sum_{\lambda \in \Lambda} \sum_{k=1}^{K} \|\lambda_k - m_K\|^2 P(\lambda) \approx G_L(1 + 2/L) (N\nu)^{2/L} \frac{\int_{y \in \Omega_0} \sum_{k=1}^{K-1} y_k^{2/L} \, dy}{\int_{y \in \Omega_0} dy}. \tag{4.15}$$

Let $V(\Omega_0)$ denote the volume of region Ω_0, then

$$\begin{aligned} V(\Omega_0) &= \int_{y \in \Omega_0} dy_1 \, dy_2 \cdots dy_{K-1} \\ &= K^{L/2} \int_{x \in \Omega} dx_1 \, dx_2 \cdots dx_{K-1} \\ &= K^{L/2} N_\tau \\ &= K^{-L/2} N. \end{aligned} \tag{4.16}$$

Let G_{Ω_0} denote the dimensionless normalized $\frac{2}{L}$th moment of Ω_0, that is

$$G_{\Omega_0} \triangleq \frac{1}{K-1} \frac{\int_{y \in \Omega_0} \sum_{k=1}^{K-1} y_k^{2/L} \, dy}{V(\Omega_0)^{1 + \frac{2/L}{K-1}}}. \tag{4.17}$$

Applying scaling on Ω_0 will not change G_{Ω_0}, which makes it a good figure of the shape of Ω_0. For the special case $L = 1$, the region Ω_0 is a $K-1$ dimensional sphere in the first octant, so the normalized second moment $G_{\Omega_0} = 4G_{K-1}$. For the special case $K = 2$, $G_{\Omega_0} = L/(L+2)$ is the normalized $\frac{2}{L}$th moment of a line $[0, C]$. Generally, using *Dirichilet's Integral* [54], we get

$$G_{\Omega_0} = \frac{1}{n + \frac{2}{L}} \frac{\Gamma(\frac{nL}{2} + 1)^{\frac{2}{nL}}}{\Gamma(\frac{L}{2} + 1)^{\frac{2}{L}}}, \tag{4.18}$$

where the Gamma function is defined as

$$\Gamma(z) = \int_0^\infty t^{z-1} e^{-t} \, dt. \tag{4.19}$$

Hence,

$$\frac{\int_{y\in\Omega_0} \sum_{k=1}^{K-1} y_k^{2/L} \, dy}{\int_{y\in\Omega_0} dy} = G_{\Omega_0}(K-1)V(\Omega_0)^{\frac{2/L}{K-1}} = G_{\Omega_0}(K-1)K^{\frac{-1}{K-1}}N^{\frac{2/L}{K-1}}. \tag{4.20}$$

Substituting (4.20) into (4.15), we have

$$\begin{aligned}\frac{1}{K}\sum_{\lambda\in\Lambda}\sum_{k=1}^{K}\|\lambda_k - m_K\|^2 P(\lambda) &\approx G_L G_{\Omega_0}(1+2/L)(K-1)K^{\frac{-K}{K-1}}N^{\frac{K}{K-1}\frac{2}{L}}\nu^{\frac{2}{L}} \\ &\approx G_L \Phi_{K-1,L}(K-1)K^{\frac{-K}{K-1}}N^{\frac{K}{K-1}\frac{2}{L}}\nu^{\frac{2}{L}},\end{aligned} \tag{4.21}$$

where

$$\Phi_{n,L} = \frac{1+\frac{2}{L}}{n+\frac{2}{L}} \frac{\Gamma(\frac{nL}{2}+1)^{\frac{2}{nL}}}{\Gamma(\frac{L}{2}+1)^{\frac{2}{L}}}.$$

Note $\Phi_{n,1} = 12G_n$ and $\Phi_{1,L} = 1$.

Comparing (4.9) with (4.21), the first term of d_s dominates the second term when $N \to \infty$, thus

$$d_s \approx G_L \Phi_{K-1,L}(K-1)K^{\frac{-K}{K-1}}N^{\frac{K}{K-1}\frac{2}{L}}\nu^{\frac{2}{L}}. \tag{4.22}$$

Substituting (4.22) and (2.7) into (2.23), we finally get a closed form solution of the expected distortion for optimal MDLVQ

$$D = (1-p^K)G_\Lambda \nu^{2/L} + \zeta_2 G_L \Phi_{K-1,L}(K-1)K^{\frac{-K}{K-1}}N^{\frac{K}{K-1}\frac{2}{L}}\nu^{\frac{2}{L}} + p^K E[\|X\|^2]. \tag{4.23}$$

The total target entropy is $R_t = KR$, so we rewrite (2.14) to get

$$N\nu = 2^{L(h(p)-R_t/K)}. \tag{4.24}$$

For simplicity, define

$$\eta \triangleq 2^{L(h(p)-R_t/K)}. \tag{4.25}$$

Now we have

$$D = (1-p^K)G_\Lambda \nu^{2/L} + \zeta_2 G_L \Phi_{K-1,L}(K-1)K^{\frac{-K}{K-1}}\eta^{\frac{K}{K-1}\frac{2}{L}}\nu^{\frac{-1}{K-1}\frac{2}{L}} + p^K E[\|X\|^2]. \tag{4.26}$$

By differentiating D to ν, we get the optimal ν.

$$\nu_{opt} = \eta \left(\frac{\zeta_2}{1-p^K} \frac{G_L}{G_\Lambda} \frac{\Phi_{K-1,L}}{K^{\frac{K}{K-1}}} \right)^{\frac{L(K-1)}{2K}}.$$

Substituting ν_{opt} to (4.24), we get optimal N:

$$N_{opt} = \left(\frac{1-p^K}{\zeta_2} \frac{G_\Lambda}{G_L} \frac{K^{\frac{K}{K-1}}}{\Phi_{K-1,L}} \right)^{\frac{L(K-1)}{2K}}. \tag{4.27}$$

If $K = 2$, the expression of N_{opt} can be simplified as

$$N_{opt} = \left(\frac{2(1+p)}{p} \frac{G_\Lambda}{G_L} \right)^{\frac{L}{4}}. \tag{4.28}$$

Remark 1: N_{opt} is independent of the total target entropy rate R_t and source entropy rate $h(p)$. It only depends on the loss probability p and on the number of descriptions K. Substituting ν_{opt} into (4.26), the average distortion can be expressed as a function of K. Then optimal K can be solved numerically.

Remark 2: When $K = 2$, (4.22) can be simplified to

$$d_s \approx \frac{1}{4} G_L (N^2 \nu)^{2/L}. \tag{4.29}$$

For any $a \in (0,1)$, let $N = 2^{L(aR+1)}$, then $\nu = 2^{L(h(p)-(a+1)R-1)}$. Note when $R \to \infty$, we have $N \to \infty$. Substituting the expressions of N and ν in to (2.7) and (4.29), we

get

$$\lim_{R\to\infty} d_c 2^{2R(1+a)} = \frac{1}{4} G_\Lambda 2^{2h(p)}$$

$$\lim_{R\to\infty} d_i 2^{2R(1-a)} = G_L 2^{2h(p)}, \quad i = 1, 2$$

So asymptotically, the proposed algorithm achieves the second-moment gain of a lattice for the central distortion, and the second-moment gain of a sphere for the side distortion, thus the asymptotic performance is optimal and the same as the expression in [51].

Chapter 5

Codecell Convexity of MDSQ

In this chapter we study the relationship between the optimality of multiple description scalar quantizers (MDSQ) and the convexity of the side quantizers of MDSQ. The significance of this study is two folds: first, the codecell convexity or lack of it reveals the structures of optimal MDSQ; second, constraining the side quantizers to be convex can greatly simplify optimal MDSQ design [13].

We say that a scalar quantizer is convex if all its codecells are contiguous intervals on the real line (i.e., a convex point set). For fixed-rate single description scalar quantization, constraining the codecells to be convex does not preclude optimality [18]. In the case of entropy-constrained single description scalar quantization, the optimality of a scaler quantizer design requires codecell convexity only for continuous sources, but not so for discrete sources [25]. Effros *et al.* showed that codecell convexity of side quantizers can preclude optimality for some discrete distributions in

both fixed-rate and entropy-constrained MDSQ [14]. Dumitrescu and Wu investigated the conditions in which optimal MDSQ have convex side quantizers [12].

Although globally optimal single description scalar quantizer design can be solved in polynomial time [55], no polynomial-time algorithm for optimal MDSQ design has so far been proposed, nor has the problem been proven to be NP-complete.

Vaishampayan proposed a local optimization approach of gradient descent to MDSQ design [48]. However, the problem of optimal MDSQ is solvable in polynomial time complexity if the side quantizers are confined to be convex [13, 12, 33, 14]. That is why we are interested in the convexity of MDSQ.

5.1 Measurement of Convexity

Each codeword of the central quantizer of MDSQ is a central lattice point λ. The corresponding codecell (central cell) is the Voronoi cell $V(\lambda)$, and hence is convex. The codecell of side quantizer (side cell) k ($k \in \{1, 2, \cdots, K\}$) for a sublattice point λ_s, is

$$W_k(\lambda_s) = \bigcup_{\alpha_k(\lambda)=\lambda_s} V(\lambda) \tag{5.1}$$

Since the codecell of a side quantizer is the union of several central quantizer cells, it may not be convex (i.e., the union is not necessarily a contiguous interval on the real line). In order to measure the degree of convexity of the side quantizer $W_k(\lambda_s)$, we

define a cell compactness factor:

$$C_k(\lambda_s) = \frac{Vol(W_k(\lambda_s))}{Vol(Convexhull(W_k(\lambda_s)))}. \tag{5.2}$$

If $W_k(\lambda_s)$ is convex, $C_k(\lambda_s) = 1$. In general, it is between 0 and 1.

For MDSQ with lattice code books, central cells are intervals with equal length ν. Those central cells are ordered in real line $(-\infty, \infty)$. Let the central lattice be $\Lambda = \{\cdots, x_{-2}, x_{-1}, x_0, x_1, x_2, \cdots\} = \{\cdots, -2\nu, -\nu, 0, \nu, 2\nu, \cdots\}$, where $x_i = i\nu$. Let the sublattice be $\Lambda_s = \{\cdots, y_{-2}, y_{-1}, y_0, y_1, y_2, \cdots\} = \{\cdots, -2\nu N, -\nu N, 0, \nu N, 2\nu N, \cdots\}$, where $y_i = i\nu N$. We can see that the central cell $V(x_i) = [(i - \frac{1}{2})\nu, (i + \frac{1}{2})\nu)$.

A side cell is jointed by several central cells. It can be a contiguous interval (if it is convex) or the union of several disjoint intervals (if it is not convex). Define the spread of a side cell $W_k(\lambda_s)$, $k \in \{1, 2, \cdots, K\}$ as

$$S_k(\lambda_s) = \frac{max(W_k(\lambda_s)) - min(W_k(\lambda_s))}{\nu}. \tag{5.3}$$

The definition of spread is equivalent to that in [48]. It follows that $S_k(\lambda_s)$ is an integer. And latter we will show

$$C_k(\lambda_s) = \frac{N}{S_k(\lambda_s)}. \tag{5.4}$$

5.2 Index Assignment Matrix

An index assignment of MDSQ can be expressed by an index assignment (IA) matrix. Assume an index assignment function α maps a central lattice point x_l to an

ordered K-tuple: $\alpha(x_l) = (y_{i_1}, y_{i_2}, \cdots, y_{i_K})$. Then the index assignment function can be represented by a K dimensional IA matrix, where each integer l is placed in $(i_1, i_2, \cdots, i_K)$.

For convenience of drawing pictures, we assume $K = 2$ so that the IA matrix is two dimensional. If the index assignment maps x_l to an ordered pair (y_i, y_j): $\alpha(x_l) = (y_i, y_j)$, the integer l is placed in row i and column j of the associated IA matrix.

At first, we assume that N is odd. When N is odd, the sublattice is clean, centric and S-similar to the central lattice, thus the greedy IA algorithm is optimal (Theorem 1). There is an odd number of central lattice points in $V_{s/2}(\tau)$, if $\tau \in \Lambda_s$. Their index assignments are represented by the blocks with odd elements spreading from the matrix diagonal in Figure 5.1. There is an even number of central lattices in $V_{s/2}(\tau)$, if $\tau \notin \Lambda_s$. Their index assignments are represented by the blocks with even elements spreading from the matrix diagonal. The greater the sublattice index N, the wider the spread of the indices away from the main diagonal. This corresponds to different trade-offs between the central and side distortions.

Figure 5.2 shows the index assignments obtained by the greedy algorithm for $N = 3$. $V_{s/2}(O)$ has one central lattice point x_0, which is labeled by (O, O): $\alpha(x_0) = (O, O)$; $V_{s/2}(\frac{O+A}{2})$ has two central lattice points x_1, x_2, which are labeled by (A, O) and (O, A) respectively: $\alpha(x_1) = (A, O), \alpha(x_2) = (O, A)$. Figure 5.3 (a) shows the associated IA matrix of Figure 5.2. By switching the index assignments for x_1, x_2, we

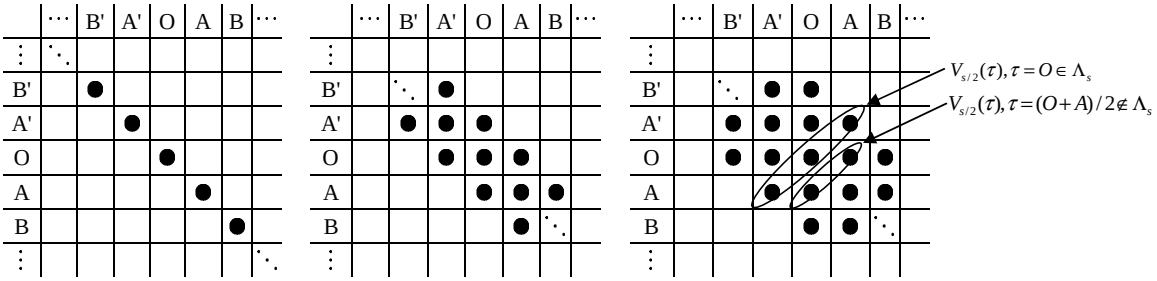

(a) $N = 1$ (b) $N = 3$ (c) $N = 5$

Figure 5.1: Selected index pairs for different values of N.

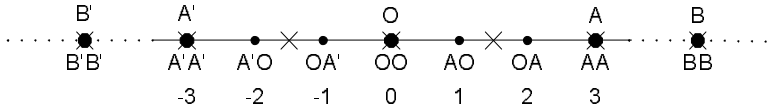

Figure 5.2: Index assignments for $N = 3$. Points of Λ, Λ_s and $\Lambda_{s/2}$ are marked by $\cdot$, $\bullet$, and $\times$, respectively.

have $\alpha(x_1) = (O, A), \alpha(x_2) = (A, O)$. This is shown in Figure 5.3 (b). The switching does not affect the average distortion D as discussed in Section 3.2. However, after switching, the maximum spread increase from 4 in Figure 5.3 (a) to 5 in Figure 5.3 (b). Thus the maximum side distortion increases by switching, which is usually not favorable.

When N is even, the sublattice is not clean. But it is easy to show the greedy algorithm is still optimal if we broke the tie on the boundary of a Voronoi cell of the K-fraction lattice. Index assignments for other values of N are illustrated in Figure 5.4 and Figure 5.5. Those index assignments are given by our greedy index assignment algorithm in Section 3.2, with additional criteria of minimizing the maximum side

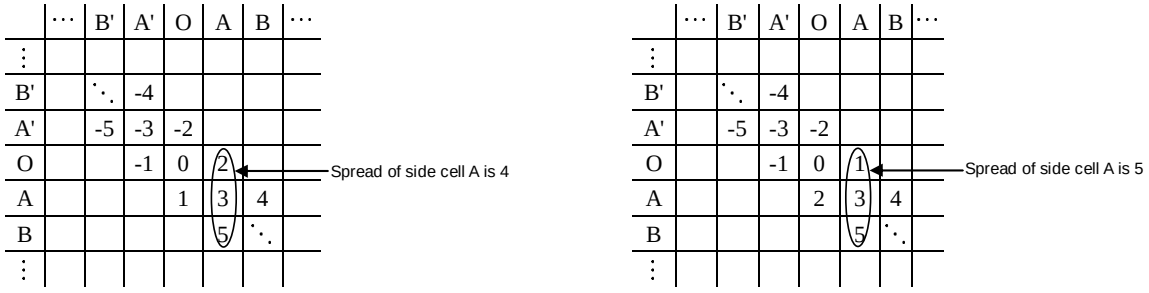

(a) IA matrix for Figure 5.2 (b) IA matrix after switching

Figure 5.3: IA matrices for $N = 3$. (a) and (b) show two optimal index assignments with different spreads

distortion (or spread). Vaishampayan presented good index assignments for odd N in his pioneer work on MDSQ [48]. The IA matrices in [48] is given by intuition without proof of optimality. Interestingly, his IA matrices are the same as our optimal IA matrices for MDSQ with lattice codebooks.

5.3 Compactness of Side Cells vs. Probability of Packet Loss

The expected distortion of optimal two-description MDLVQ is denoted by (4.7), which holds for MDSQ with Z lattice codebooks and odd N (because the the sublattice of Z lattice is clean, S-similar and centric when N is odd). The expected distortion of our optimal greedy algorithm for MDSQ with Z lattice and even N is easy to deduct

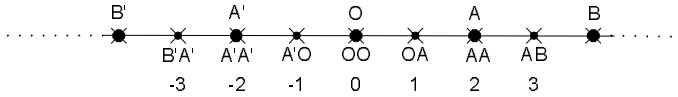

(a) $N = 2$

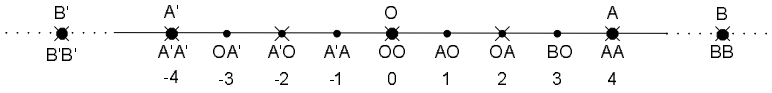

(b) $N = 4$

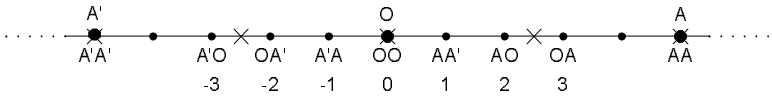

(c) $N = 5$

Figure 5.4: Index assignments for $N = 2, 4, 5$. Points of Λ, Λ_s and $\Lambda_{s/2}$ are marked by $\cdot$, $\bullet$, and $\times$, respectively.

and omitted here. The results are

$$D = \begin{cases} \frac{1}{12}(1-p^2)\nu^2 + \frac{1}{24}p(1-p)(N^4-1)\nu^2 + p^2E[\|X\|^2], & N \equiv 1 \bmod 2, \\ \frac{1}{12}(1-p^2)\nu^2 + \frac{1}{24}p(1-p)(N^4+3N^2+8)\nu^2 + p^2E[\|X\|^2], & N \equiv 0 \bmod 4, \\ \frac{1}{12}(1-p^2)\nu^2 + \frac{1}{24}p(1-p)(N^4+3N^2-4)\nu^2 + p^2E[\|X\|^2], & N \equiv 2 \bmod 4. \end{cases}$$

The optimal sublattice index N_* versus the description loss probability p is shown in Figure 4.2.

Given N, any side cell has the same spread $\frac{N^2-N}{2}+1$, and compactness $\frac{N}{\frac{N^2-N}{2}+1} = \frac{2N}{N^2-N+2}$. If p is greater than $\frac{5}{47} = \%10.6$, the optimal sublattice index $N_* \leq 2$, thus optimal side quantizers has convex codecells. Figure 5.6 shows the compactness of side cells versus probability of description loss.

	⋯	B'	A'	O	A	B	⋯
⋮	⋱						
B'		-4	-3				
A'			-2	-1			
O				0	1		
A					2	3	
B						4	
⋮							⋱

(a) $N = 2$

	⋯	B'	A'	O	A	B	⋯
⋮							
B'		⋱	-6	-5			
A'		-7	-4	-2	-1		
O			-3	0	2	3	
A				1	4	6	
B					5	⋱	
⋮							

(b) $N = 4$

	⋯	B'	A'	O	A	B	⋯
⋮							
B'		⋱	-7	-6			
A'		-8	-5	-3	-1		
O		-4	-2	0	3	6	
A			1	2	5	7	
B				4	8	⋱	
⋮							

(c) $N = 5$

Figure 5.5: IA matrices for $N = 2, 4, 5$.

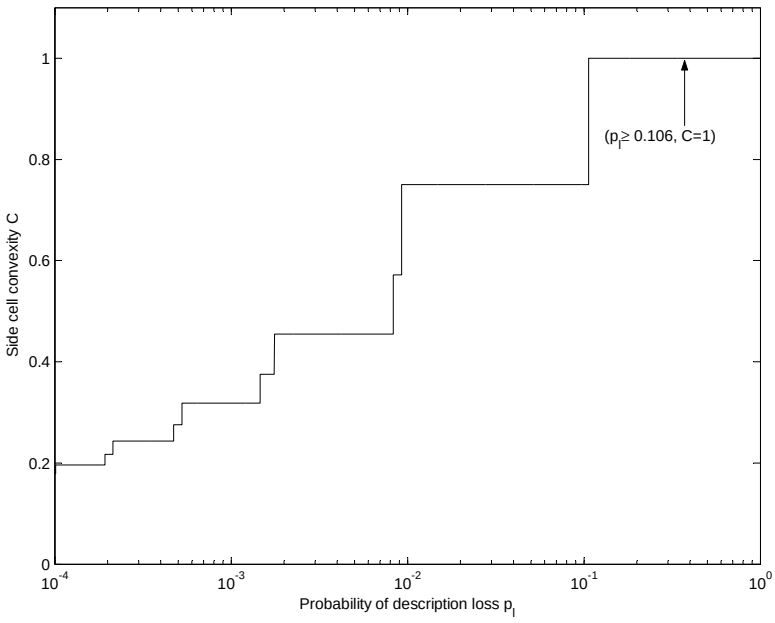

Figure 5.6: Compactness of side cells versus description loss probability p.

Chapter 6

Conclusions

Multiple description lattice vector quantization is a promising technique for robust networked signal communications. Optimal index assignment is a key issue in MDLVQ design that largely determines the rate-distortion performance of the system. Although optimal MDLVQ index assignment is conceptually a problem of linear assignment, the challenge is that the original problem involves a bijective mapping between two infinite sets Λ and Λ_s^K. No good solutions are known to reduce the underlying bipartite graph to a modest size while ensuring optimality. Therefore, the problem remains largely open. This thesis presented a linear-time algorithm for optimal MDLVQ index assignment. Under some mild conditions, the algorithm is optimal for two balanced descriptions in any dimensions and for any sublattice index values N. We conjecture that the algorithm, with an appropriate local adjustment, is also optimal for any number of balanced descriptions K.

We also made progress in the analysis of MDLVQ performance. Exact closed form expression of the expected distortion was derived for $K = 2$ and for any N. For cases $K > 2$, we improved the current asymptotic ($N \to \infty$) expression of the expected distortion.

Bibliography

[1] R. Balan, I. Daubechies, and V. Vaishampayan. The analysis and design of windowed fourier frame based multiple description source coding schemes. *IEEE Trans. Inform. Theory*, 46(7):2491 – 2536, Nov. 2000.

[2] J. Balogh and J. A. Csirik. Index assignment for two-channel quantization. *IEEE Trans. Inform. Theory*, 50(11):2737–2751, Nov 2004.

[3] T. Berger. *Rate Distortion Theory: A Mathematical Basis for Data Compression.* Prentice-Hall, Englewood Cliffs, 1971.

[4] T. Y. Berger-Wolf and E. M. Reingold. Index assignment for multichannel communication under failure. *IEEE Trans. Inform. Theory*, 48(10):2656–2668, Oct. 2002.

[5] J. Cardinal. Design of tree-structured multiple description vector quantizers. In *Proc. IEEE Data Compression Conf.*, pages 23–32, Mar. 2001.

[6] J. H. Conway and N. J. A. Sloane. Fast quantizing and decoding and algorithms for lattice quantizers and codes. *IEEE Trans. Inform. Theory*, 28(2):227–232, Mar 1982.

[7] J. H. Conway and N. J. A. Sloane. A fast encoding method for lattice codes and quantizers. *IEEE Trans. Inform. Theory*, 29(6):820 – 824, Nov. 1983.

[8] J. H. Conway and N. J. A. Sloane. *Sphere Packings, Lattices, and Groups*. Springer, 1998.

[9] T. Cover and J. Thomas. *Elements of Information Theory*. Wiley and Sons, New York, 1991.

[10] S. N. Diggavi, N. J. A. Sloane, and V. A. Vaishampayan. Design of asymmetric multiple description lattice vector quantizers. In *Proc. IEEE Data Compression Conf.*, pages 490–499, Mar. 2000.

[11] S. N. Diggavi, N. J. A. Sloane, and V. A. Vaishampayan. Asymmetric multiple description lattice vector quantizers. *IEEE Trans. Inform. Theory*, 48(1):174–191, Jan. 2002.

[12] S. Dumitrescu and X. Wu. On global optimality of generalized lloyd-type algorithms for fixed-rate multiple description scalar quantizer design. *submitted to IEEE Transactions on Information Theory*, 2005.

[13] S. Dumitrescu and X. Wu. Optimal two-description scalar quantizer design. *Algorithmica*, 41(4):269–287, Feb. 2005.

[14] M. Effros and D. Muresan. Codecell contiguity in optimal fixed-rate and entropy-constrained network scalar quantizers. In *Proc. IEEE Data Compression Conf.*, pages 312–321, Apr. 2002.

[15] M. Fleming and M. Effros. Generalized multiple description vector quantization. In *Proc. IEEE Data Compression Conf.*, pages 3–12, Mar. 1999.

[16] A. A. E. Gamal and T. Cover. Achievable rates for multiple descriptions. *IEEE Transactions on Information Theory*, 28(6):851–857, Nov. 1982.

[17] M. Garey, D. S. Johnson, and H. S. Witsenhausen. The complexity of the generalized lloydcmax problem. *IEEE Trans. Inform. Theory*, 28(2):255C266, Mar. 1982.

[18] A. Gersho and R. M. Gray. *Vector Quantization and Signal Compression*. Kluwer Academic Publishers, 1992.

[19] H. Gish and J. N. Pierce. Asymptotically efficient quantizing. *IEEE Trans. Inform. Theory*, 14(5):676– 683, Sep. 1968.

[20] N. Gortz and P. Leelapornchai. Optimization of the index assignments for multiple description vector quantizers. *IEEE Trans. Commun.*, 51(3):336–340, Mar. 2003.

[21] V. K. Goyal. Multiple description coding: compression meets the network. *IEEE Signal Processing Mag.*, pages 74–93, Sep. 2001.

[22] V. K. Goyal, J. A. Kelner, and J. Kovačević. Multiple description vector quantization with a coarse lattice. *IEEE Trans. Inform. Theory*, 48:781–788, Mar. 2002.

[23] V. K. Goyal and J. Kovačević. Generalized multiple descriptions coding with correlating transforms. *IEEE Trans. Inform. Theory*, 47(6):2199–2224, Sep. 2001.

[24] R. M. Gray and D. Neuhoff. Quantization. *IEEE Trans. Inform. Theory*, 44:2325–2383, Oct. 1998.

[25] A. Gyorgy and T. Linder. On the structure of optimal entropy-constrained scalar quantizers. *IEEE Transactions on Information Theory*, 48:416–427, Feb 2002.

[26] J. Hopcroft and R. Karp. An $O(n^{5/2})$ algorithm for maximum matchings in bipartite graphs. *SIAM Journal on Computing*, 2(4):225–231, 1973.

[27] X. Huang and X. Wu. Optimal index assignment for multiple description lattice vector quantization. In *Proc. IEEE Data Compression Conf.*, pages 272 – 281, Mar. 2006.

[28] H. Jafarkhani and V. Tarokh. Multiple description trellis-coded quantization. *IEEE Trans. Commun.*, 47(6):799 C 803, Jun. 1999.

[29] N. S. Jayant. Subsampling of a dpcm speech channel to provide two 'self-contained' half-rate channels. *Bell Syst. Tech. J.*, 60(4):501–509, Apr 1981.

[30] J. A. Kelner, V. K. Goyal, and J. Kovačević. Multiple description lattice vector quantization: Variations and extensions. In *Proc. IEEE Data Compression Conf.*, pages 480–489, Mar. 2000.

[31] J. Kovačević, P. L. Dragotti, and V. K. Goyal. Filter bank frame expansions with erasures. *IEEE Trans. Inform. Theory*, 48(6):1439–1450, Jun. 2002.

[32] T. Linder and R. Zamir. On the asymptotic tightness of the shannon lower bound. *IEEE Transactions on Information Theory*, 40(6):2026–2031, Nov 1994.

[33] D. Muresan and M. Effros. Quantization as histogram segmentation: globally optimal scalar quantizer design in network systems. In *Proc. IEEE Data Compression Conf.*, pages 302 – 311, Apr. 2002.

[34] M. T. Orchard, Y. Wang, V. Vaishampayan, and A. R. Reibman. Redundancy ratedistortion analysis of multiple description coding using pairwise correlating transforms. In *Proc. IEEE Conf. on Image Proc.*, volume 1, pages 608 – 611, 1997.

[35] J. Østergaard, J. Jensen, and R. Heusdens. n-channel symmetric multiple-description lattice vector quantization. In *Proc. IEEE Data Compression Conf.*, pages 378–387, Mar. 2005.

[36] J. Østergaard, J. Jensen, and R. Heusdens. n-channel entropy-constrained multiple-description lattice vector quantization. *IEEE Trans. Inform. Theory*, 52(5):1956–1973, May 2006.

[37] L. Ozarow. On a source-coding problem with two channels and three receivers. *Bell Syst. Tech. J.*, 59:1909–1921, Dec. 1980.

[38] S. S. Pradhan, R. Puri, and K. Ramchandran. n-channel symmetric multiple descriptions-part i: (n, k) source-channel erasure codes. *IEEE Trans. Inform. Theory*, 50(1):47–61, Jan. 2004.

[39] R. Puri, S. S. Pradhan, and K. Ramchandran. n-channel multiple descriptions: Theory and constructions. In *Data Compression Conf.*, pages 262 – 271, April 2002.

[40] S. D. Servetto, V. A. Vaishampayan, and N. J. A. Sloane. Multiple description lattice vector quantization. In *IEEE Proc. Data Compression Conf.*, pages 13–22, Mar. 1999.

[41] C. E. Shannon. A mathematical theory of communication. *Bell System Technical Journal*, 27:379–423 and 623–656, July and October 1948.

[42] C. E. Shannon. Coding theorems for a discrete source with a fidelity criterion. *IRE National Convention Record*, 7(4):142–163, 1959.

[43] C. Tian and S. Hemami. Sequential design of multiple description scalar quantizers. In *IEEE Data Compression Conference*, pages 32–42, 2004.

[44] C. Tian and S. S. Hemami. A special class of multiple description scalar quantizers. In *Information Theory Workshop*, pages 24–29, Oct. 2004.

[45] C. Tian and S. S. Hemami. Universal multiple description scalar quantization: analysis and design. *IEEE Transactions on Information Theory*, 50(9):2089 C 2102, Sep. 2004.

[46] C. Tian and S. S. Hemami. Staggered lattices in multiple description quantization. In *Proc. IEEE Data Compression Conf.*, pages 398–407, Mar. 2005.

[47] V. Vaishampayan and J.-C. Batllo. Asymptotic analysis of multiple description quantizers. *IEEE Trans. Inform. Theory*, 44(1):278–284, Jan 1998.

[48] V. A. Vaishampayan. Design of multiple description scalar quantizers. *IEEE Trans. Inform. Theory*, 39:821–834, May 1993.

[49] V. A. Vaishampayan, J. C. Batllo, and A. R. Calderbank. On reducing granular distortion in multiple description. In *IEEE Int. Symp. Information Theory*, page 98, Aug. 1998.

[50] V. A. Vaishampayan and J. Domaszewicz. Design of entropy-constrained multiple-description scalar quantizers. *IEEE Trans. Inform. Theory*, 40:245–250, Jan. 1994.

[51] V. A. Vaishampayan, N. J. A. Sloane, and S. D. Servetto. Multiple description vector quantization with lattice codebooks: Design and analysis. *IEEE Trans. Inform. Theory*, 47(5):1718–1734, July 2001.

[52] R. Venkataramani, G. Kramer, and V. Goyal. Multiple description coding with many channels. *IEEE Trans. Inform. Theory*, 49(9):2106–2114, Sep. 2003.

[53] X. Wang and M. T. Orchard. Multiple description coding using trellis coded quantization. *IEEE Trans. Image Proc.*, 1:391 C 394, Sep. 2001.

[54] E. T. Whittaker and G. N. Watson. *A Course of Modern Analysis*. Camb. Univ. Press, 4th edition, 1963.

[55] X. Wu. Optimal quantization by matrix searching. *J. Algorithms*, 12(4):663–673, Dec. 1991.

[56] P. Zador. Asymptotic quantization error of continuous signals and the quantization dimension. *IEEE Trans. Inform. Theory*, 28:139–149, Mar. 1982.

[57] R. Zamir. Gaussian codes and shannon bounds for multiple descriptions. *IEEE Trans. Inform. Theory*, 45:2629–2635, Nov. 1999.

[58] Z. Zhang and T. Berger. New results in binary multiple descriptions. *IEEE Transactions on Information Theory*, 33(4):502–521, July 1987.

[59] D. Y. Zhao and W. B. Kleijn. Multiple-description vector quantization using translated lattices with local optimization. In *Global Telecommunications Conference*, volume 1, pages 41– 45, 2004.